

**Co-Editor Decision: Publish subject to technical corrections (05 Dec 2016) by Dr. Jens-Uwe Grooß**

We thank Dr. Grooß for considering our paper for publication. Below we provide a detailed point-by-point answer (AC – Author Comment) to the remaining technical issues on our manuscript (CEC – Co-Editor Comment).

**CEC:**

**Comments to the Author:**

**Dear Authors,**

**thank you for the revision. I am happy to accept your paper for publication in ACP. There are few remaining technical issues that I recognized:**

**p 12, line 19: change to "builds up"**

**AC:**

The typo has been corrected.

**CEC:**

**p 18, line 10: remove/replace html code**

**AC:**

The typo has been corrected.

**CEC:**

**table 2 footnote b: change to "given as wavenumber  $\nu/c$  in  $\text{cm}^{-1}$ "**

**(suggested by the reviewer, but not changing the numbers in the table; not all readers are spectrocopists)**

**AC:**

Table 2 footnote b has been changed to “given as wavenumber in  $\text{cm}^{-1}$ ”

1 **Nighttime atmospheric chemistry of iodine**

2 Alfonso Saiz-Lopez<sup>1</sup>, John M.C. Plane<sup>2</sup>, Carlos A. Cuevas<sup>1</sup>, Anoop S. Mahajan<sup>3</sup>, Jean-François  
3 Lamarque<sup>4</sup> and Douglas E. Kinnison<sup>4</sup>

4 <sup>1</sup>Department of Atmospheric Chemistry and Climate, Institute of Physical Chemistry  
5 Rocasolano, CSIC, Madrid, Spain

6  
7 <sup>2</sup>School of Chemistry, University of Leeds, Leeds, UK

8  
9 <sup>3</sup>Indian Institute of Tropical Meteorology, Pune, India

10  
11 <sup>4</sup>Atmospheric Chemistry Observations and Modelling, NCAR, Colorado, USA

12 Correspondence to: A. Saiz-Lopez (a.saiz@csic.es)

1 **Abstract**

2 Little attention has so far been paid to the nighttime atmospheric chemistry of iodine species.  
3 Current atmospheric models predict a buildup of HOI and I<sub>2</sub> during the night that leads to a spike  
4 of IO at sunrise, which is not observed by measurements. In this work, electronic structure  
5 calculations are used to survey possible reactions that HOI and I<sub>2</sub> could undergo at night in the  
6 lower troposphere, and hence reduce their nighttime accumulation. The new reaction NO<sub>3</sub> + HOI  
7 → IO + HNO<sub>3</sub> is proposed, with a rate coefficient calculated from statistical rate theory over the  
8 temperature range 260 - 300 K and at a pressure of 1000 hPa to be  $k(T) = 2.7 \times 10^{-12} (300 \text{ K} / T$   
9  $)^{2.66} \text{ cm}^3 \text{ molecule}^{-1} \text{ s}^{-1}$ . This reaction is included in two atmospheric models, along with the  
10 known reaction between I<sub>2</sub> and NO<sub>3</sub>, to explore a new nocturnal iodine radical activation  
11 mechanism. The results show that this iodine scheme leads to a considerable reduction of  
12 nighttime HOI and I<sub>2</sub>, which results in the enhancement of more than 25% of nighttime ocean  
13 emissions of HOI + I<sub>2</sub> and the removal of the anomalous spike of IO at sunrise. We suggest that  
14 active nighttime iodine can also have a considerable, so far unrecognized, impact on the  
15 reduction of the NO<sub>3</sub> radical levels in the marine boundary layer (MBL) and hence upon the  
16 nocturnal oxidizing capacity of the marine atmosphere. The effect of this is exemplified by the  
17 indirect effect on dimethyl sulfide (DMS) oxidation.

18

19

20

21

## 1 **1. Introduction**

2 Active nighttime iodine chemistry was first evidenced a decade ago when it was shown that  
3 nocturnal  $I_2$  emitted by macroalgae could react with  $NO_3$  leading to the formation of IO and  
4 OIO, which were measured in the coastal MBL at Mace Head, Ireland (Saiz-Lopez and Plane,  
5 2004). The nitrate radical has also been recently suggested as a nocturnal loss of  $CH_2I_2$ , which  
6 helps to reconcile observed and modelled concentrations of this iodocarbon over the remote  
7 MBL (Carpenter et al., 2015). However, most of the work on reactive atmospheric iodine has  
8 focused on the use of daytime observations and models to assess its role in the catalytic  
9 destruction of ozone and the oxidizing capacity of the troposphere (e.g. Saiz-Lopez et al. (2012b)  
10 and references therein). In the MBL, iodine-, along with bromine-catalysed ozone destruction  
11 contributes up to 45% of the observed daytime depletion (Read et al., 2008; Mahajan et al.,  
12 2010a), although this contribution shows large geographical variability (Mahajan et al., 2012;  
13 Gómez Martín et al., 2013; Prados-Roman et al., 2015b; Volkamer et al., 2015). Iodine  
14 compounds have also been implicated in the formation of aerosols, although the mechanisms and  
15 magnitudes of these processes are not fully understood (Hoffmann et al., 2001; O'Dowd et al.,  
16 2002; McFiggans et al., 2004; Gomez Martin et al., 2013; Allan et al., 2015; Roscoe et al., 2015).  
17 Reactive forms of inorganic iodine may also contribute to the oxidation of elemental mercury  
18 over the tropical oceans (Wang et al., 2014). In recent years, iodine sources and chemistry have  
19 also been implemented in global models demonstrating the effect of iodine chemistry in the  
20 oxidation capacity of the global marine troposphere (Ordóñez et al., 2012; Saiz-Lopez et al.,  
21 2012a; Saiz-Lopez et al., 2014; Sherwen et al., 2016).

22 Iodine is emitted into the atmosphere from the ocean surface in both organic and inorganic  
23 forms. The main organic compounds emitted are methyl iodide ( $CH_3I$ ), ethyl iodide ( $C_2H_5I$ ),

1 propyl iodide (1- and 2-C<sub>3</sub>H<sub>7</sub>I), chloriodomethane (CH<sub>2</sub>ICl), bromiodomethane (CH<sub>2</sub>IBr), and  
2 diiodomethane (CH<sub>2</sub>I<sub>2</sub>) (Carpenter, 2003; Butler et al., 2007; Jones et al., 2010; Mahajan et al.,  
3 2012). However, these organic compounds contribute only up to a fourth of the MBL iodine  
4 loading (Jones et al., 2010; Mahajan et al., 2010a; Großmann et al., 2013; Prados-Roman et al.,  
5 2015b). Inorganic emissions of HOI and I<sub>2</sub>, which result from the deposition of O<sub>3</sub> at the ocean  
6 surface and subsequent reaction with I<sup>-</sup> ions in the surface microlayer, account for the main  
7 source of iodine in the MBL (Carpenter et al., 2013). Recent laboratory experiments have shown  
8 that HOI is the major compound emitted, and provided parameterizations of the fluxes of both  
9 species depending on wind speed, temperature, and the concentrations of O<sub>3</sub> and I<sup>-</sup> (Carpenter et  
10 al., 2013; MacDonald et al., 2014). These parameterized fluxes of HOI and I<sub>2</sub> have then been  
11 used in a one-dimensional model to study the diurnal evolution of the IO and I<sub>2</sub> mixing ratios at  
12 the Cape Verde Atmospheric Observatory (CVAO) (Carpenter et al., 2013; Lawler et al., 2014).  
13 The model simulations replicate well the levels and general diurnal profiles of IO and I<sub>2</sub>,  
14 although an early morning ‘dawn spike’ in IO is predicted by the models, but has not been  
15 observed (Read et al., 2008; Mahajan et al., 2010a). The morning peak predicted by current  
16 iodine chemistry models is due to a buildup of the emitted I<sub>2</sub> and HOI (which is converted into  
17 IBr/ICl through heterogeneous sea-salt recycling) over the course of the night, followed by rapid  
18 photolysis at sunrise.

19 Traditionally it has been thought that iodine chemistry has a negligible effect on oxidizing  
20 capacity of the nocturnal marine atmosphere. As a consequence, unlike the demonstrated effect  
21 of iodine on the levels of daytime oxidants, the impact of active iodine upon the main nighttime  
22 oxidant, NO<sub>3</sub>, remains an open question. This is important given that in many parts of the ocean  
23 the NO<sub>3</sub> + DMS reaction is at least as important as OH + DMS in oxidizing DMS (Allan et al.,

1 2000), and hence a reduction of NO<sub>3</sub> may have an effect in the production of SO<sub>2</sub> and methane  
2 sulfonic acid (MSA). Here, we discuss possible mechanisms of nighttime iodine radical  
3 activation and their potential effect on nighttime iodine ocean fluxes and the currently modeled  
4 dawn spike in IO. A new reaction of HOI with NO<sub>3</sub> is proposed, supported by theoretical  
5 calculations. We explore the implications of this new reaction both for iodine and NO<sub>3</sub>  
6 chemistries.

7

## 8 **2. Nocturnal iodine radical activation mechanism**

9 We use the reaction mechanism that has recently been described in the global modelling studies  
10 by Saiz-Lopez et al. (2014) and (Ordóñez et al., 2012) (see supplementary information). In  
11 addition to the reactions included in that scheme, we also include nighttime gas-phase reactions  
12 based on the theoretical calculations described below. The additional reactions are listed in Table  
13 1 and a scheme with this new nocturnal chemistry is included in Figure 1.

14 To the best of our knowledge, reactions of HOI specific to night time have not been studied,  
15 either theoretically or through laboratory experiments. Currently, HOI is thought to build up  
16 overnight until sunrise, with only heterogeneous uptake on seasalt aerosol as a nighttime loss  
17 process (Saiz-Lopez et al., 2012b; Simpson et al., 2015). In addition to the well known I<sub>2</sub> + NO<sub>3</sub>  
18 reaction (R1) (Chambers et al., 1992), here we consider several possible HOI reactions that could  
19 occur at night, in the absence of photolysis and OH:





2

### 3 **3. Theoretical calculations**

4 In order to explore the feasibility of reactions 2–4 taking place under the conditions of the lower  
5 troposphere, we carried out electronic structure calculations using the hybrid density  
6 functional/Hartree-Fock B3LYP method from within the Gaussian 09 suite of programs (Frisch  
7 et al., 2009), combined with a G2 level basis set for I (Glukhovtsev et al., 1995) and the standard  
8 6-311+g(2d,p) triple zeta basis set for O, N and H. Following geometry optimizations of the  
9 relevant points on the potential energy surfaces, and the determination of their corresponding  
10 vibrational frequencies and (harmonic) zero-point energies, energies relative to the reactants  
11 were obtained at the same level of theory. Spin-orbit corrections of -30.0 (Mečiarová et al.,  
12 2011), -14.4 (Khanniche et al., 2016), -5.9 (Šulková et al., 2013) and -4.8 (Kaltsoyannis and  
13 Plane, 2008)  $\text{kJ mol}^{-1}$  were applied to the energies of I, IO, HOI and  $\text{IONO}_2$ , respectively.

14 Reaction 2 is endothermic by  $2.6 \text{ kJ mol}^{-1}$  and so, within the expected error of  $\pm 10 \text{ kJ mol}^{-1}$  at  
15 this level of theory, might be reasonably fast. However, the transition state of the reaction, which  
16 is illustrated in Figure 2(a), is  $73 \text{ kJ mol}^{-1}$  above the reactants and so this reaction will not occur  
17 at tropospheric temperatures. Reaction 3 is exothermic by  $19.8 \text{ kJ mol}^{-1}$ . An HOI--HNO<sub>3</sub>  
18 complex first forms (Figure 2(b)), which is  $21 \text{ kJ mol}^{-1}$  below the reactants. However, this  
19 complex re-arranges to the  $\text{IONO}_2 + \text{H}_2\text{O}$  products via the cyclic transition state shown in Figure  
20 2(c), which is  $110 \text{ kJ mol}^{-1}$  above the reactants.

21 The stationary points on the potential energy surface (PES) for reaction 4 are illustrated in Figure  
22 3. HOI and  $\text{NO}_3$  associate to form a complex which is  $24 \text{ kJ mol}^{-1}$  below the reactant entrance

1 channel. H-atom transfer involves a submerged transition state to form an IO--HNO<sub>3</sub> complex,  
2 which can then dissociate to the products IO + HNO<sub>3</sub>. The vibrational frequencies, rotational  
3 energies and geometries (in Cartesian co-ordinates) of these intermediates are listed in Table 2.  
4 Overall, the reaction is exothermic by 14 kJ mol<sup>-1</sup>. The energies of the HOI--NO<sub>3</sub> complex and  
5 the transition state are assigned the same spin-orbit correction as HOI (-5.9 kJ mol<sup>-1</sup> (Šulková et  
6 al., 2013)), whereas the IO--HNO<sub>3</sub> complex is assigned the spin-orbit correction of IO (-14.4 kJ  
7 mol<sup>-1</sup> (Khanniche et al., 2016)). This reflects the H-OI bond only increasing from 0.97 Å in HOI  
8 to 1.1 Å in the transition state, compared with 1.7 Å in the IO—HNO<sub>3</sub> complex. The spin-orbit  
9 correction for the transition state is therefore likely to be closer to that of HOI. Assigning the  
10 HOI spin-orbit correction therefore means that the barrier is highest with respect to the reactants,  
11 so that the estimated rate coefficient (see below) may be a lower limit.

12 The rate coefficient for reaction 4 was then estimated using Rice-Ramsperger-Kassel-Markus  
13 (RRKM) theory, employing a multi-well energy-grained master equation solver based on the  
14 inverse Laplace transform method - MESMER (Master Equation Solver for Multi-well Energy  
15 Reactions) (Roberston et al., 2014). The reaction proceeds via the formation of the excited  
16 HOI--NO<sub>3</sub> complex from HOI + NO<sub>3</sub>. This complex can then dissociate back to the reactants or  
17 rearrange to the IO--HNO<sub>3</sub> intermediate complex over the transition state, which can in turn  
18 dissociate to the products IO + HNO<sub>3</sub>. Either of the intermediates can also be stabilized by  
19 collision with the third body (N<sub>2</sub>). The time evolution of all these possible outcomes is modelled  
20 using the master equation.

21 The internal energies of the intermediates on the PES were divided into a contiguous set of  
22 grains (width 10 cm<sup>-1</sup>), each containing a bundle of rovibrational states calculated with the  
23 molecular parameters in Table 2, using the rigid-rotor harmonic oscillator approximation for all



1 species. It should be noted that the HOI--NO<sub>3</sub> and IO--HNO<sub>3</sub> complexes both have low  
2 frequency vibrational modes ( $< 100 \text{ cm}^{-1}$ ) which should more correctly be treated as hindered  
3 rotors rather than vibrations. However, in our experience this is not worth doing this until  
4 experimental rate coefficients are available to fit the rotor barrier heights. In any case, the  
5 energies of both complexes are far enough below the energy of the entrance channel (figure 3)  
6 that relatively small changes in their densities of states will have a minor effect on the overall  
7 rate coefficient. Each grain was then assigned a set of microcanonical rate coefficients linking it  
8 to other intermediates, calculated by RRKM theory. For dissociation to products or reactants,  
9 microcanonical rate coefficients were determined using inverse Laplace transformation to link  
10 them directly to the capture rate coefficient,  $k_{\text{capture}}$ . For reaction 4 and the reverse reaction IO +  
11 HNO<sub>3</sub> involving neutral species,  $k_{\text{capture}}$  was set to a typical capture rate coefficient of  $2.5 \times 10^{-10}$   
12  $(T/300 \text{ K})^{1/6} \text{ cm}^3 \text{ molecule}^{-1} \text{ s}^{-1}$ , where the small positive temperature dependence is  
13 characteristic of a long-range potential governed by dispersion and dipole-dipole forces  
14 (Georgievskii and Klippenstein, 2005).

15 The probability of collisional transfer between grains was estimated using the exponential down  
16 model, where the average energy for downward transitions was set to  $\langle \Delta E \rangle_{\text{down}} = 300 \text{ cm}^{-1}$  for  
17 N<sub>2</sub> as the third body (Gilbert and Smith, 1990). MESMER determines the temperature- and  
18 pressure-dependent rate coefficient from the full microcanonical description of the system time  
19 evolution by performing an eigenvector/eigenvalue analysis (Bartis and Widom, 1974). The  
20 resulting rate coefficient over the temperature range 260 - 300 K at a pressure of 1000 hPa is  
21  $k_4(T) = 2.7 \times 10^{-12} (300 \text{ K} / T)^{2.66} \text{ cm}^3 \text{ molecule}^{-1} \text{ s}^{-1}$ . Because the intermediate complexes are  
22 not strongly bound, and the transition state and products are below the entrance channel, the only  
23 products formed in reaction R4 under atmospheric conditions are IO + HNO<sub>3</sub>. The uncertainty in

1  $k_4$  arises principally from the estimated capture rate coefficient (see above), and the height of the  
2 barrier below the entrance channel. As discussed above, the spin-orbit correction of the transition  
3 state is likely to be larger than the value of  $-5.9 \text{ kJ mol}^{-1}$  corresponding to HOI, so  $k_4$  is possibly a  
4 lower limit. For instance, if the barrier height is decreased by  $3 \text{ kJ mol}^{-1}$ ,  $k_4$  increases by a factor  
5 of 1.9. If the barrier is lower by  $8.5 \text{ kJ mol}^{-1}$  (corresponding to the transition state having the  
6 same spin-orbit correction as IO), then  $k_4$  would increase by a factor of 5.1. Nevertheless, noting  
7 that the capture rate coefficient could be lower – perhaps by a factor of 2 - than the estimate used  
8 here, we prefer to use the value for  $k_4$  calculated with the potential surface in Figure 3. Of course,  
9 if  $k_4$  is larger, then the atmospheric impacts of reaction 4 discussed in Section 4 will be even  
10 more pronounced.

11 Note that  $\text{NO}_3$  also reacts with  $\text{CH}_2\text{I}_2$  with a rate constant  $\sim 2\text{-}4 \times 10^{-13} \text{ cm}^3 \text{ molecule}^{-1} \text{ s}^{-1}$ , which  
12 can have a significant effect on nighttime  $\text{CH}_2\text{I}_2$  concentration (Carpenter et al., 2015). However  
13 the products of this reaction are still uncertain (Nakano et al., 2006; Carpenter et al., 2015) and  
14 its rate is considerably slower than that of R4.

15 In summary, the only likely gas-phase reactions that  $\text{I}_2$  and HOI undergo in the nighttime  
16 troposphere are R1 and R4, respectively. These are included in the model reaction scheme to  
17 examine their impacts on the evolution of iodine species in the atmosphere.

18

#### 19 **4. Atmospheric modelling**

20 We use two atmospheric chemical transport models to study *i*) the impact of this new chemistry  
21 on the nighttime chemistry and partitioning of iodine species, and *ii*) the resulting geographical  
22 distribution of nocturnal iodine and impact on  $\text{NO}_3$  within the global marine boundary layer.

1 The first model, Tropospheric HAlogen chemistry MOdel (THAMO), is used for a detailed  
2 kinetics study of the impact of the different reactions shown in Table 1 as well as to assess which  
3 uptake rates best reproduce observations from a field study at the CVAO (Carpenter et al., 2011).  
4 THAMO has been used in the past to study iodine chemistry at the CVAO and further details  
5 including the full chemical scheme can be found elsewhere (Read et al., 2008; Saiz-Lopez et al.,  
6 2008; Mahajan et al., 2009; Mahajan et al., 2010a; Mahajan et al., 2010b; Lawler et al., 2014).  
7 Briefly, THAMO is a 1-D chemistry transport model with 200 stacked boxes at a vertical  
8 resolution of 5m (total height 1 km). The model treats iodine, bromine, O<sub>3</sub>, NO<sub>x</sub> and HO<sub>x</sub>  
9 chemistry, and is constrained with typical measured values of other chemical species in the  
10 MBL: [CO]=110 nmol mol<sup>-1</sup>; [DMS]=30 pmol/mol; [CH<sub>4</sub>]=1820 nmol mol<sup>-1</sup>; [ethane]=925  
11 pmol/mol; [CH<sub>3</sub>CHO]=970 pmol/mol; [HCHO]=500 pmol/mol; [isoprene]=10 pmol/mol;  
12 [propane]=60 pmol/mol; [propene]=20 pmol/mol. The average background aerosol surface area  
13 (ASA) used is 1x10<sup>-6</sup> cm<sup>2</sup> cm<sup>-3</sup> (Read et al., 2008; Lee et al., 2009; Read et al., 2009; Lee et al.,  
14 2010). The model is initialized at midnight and the evolution of iodine species, O<sub>3</sub>, NO<sub>x</sub> and HO<sub>x</sub>  
15 is followed until the model reaches steady state.

16 The second model is the global 3D chemistry-climate model CAM-Chem (Community  
17 Atmospheric Model with chemistry, version 4.0), which is used to study the impact of reactions  
18 1 and 4 on a global scale. The model includes a comprehensive chemistry scheme to simulate the  
19 evolution of trace gases and aerosols in the troposphere and the stratosphere (Lamarque et al.,  
20 2012). The model runs with the iodine and bromine chemistry schemes from previous studies  
21 (Fernandez et al., 2014; Saiz-Lopez et al., 2014; Saiz-Lopez et al., 2015), including the  
22 photochemical breakdown of bromo- and iodo-carbons emitted from the oceans (Ordóñez et al.,  
23 2012) and abiotic oceanic sources of HOI and I<sub>2</sub> (Prados-Roman et al., 2015a). CAM-Chem has

1 been configured in this work with a horizontal resolution of 1.9° latitude by 2.5° longitude and 26  
2 vertical levels, from the surface to ~40km altitude. All model runs in this study were performed  
3 in the specified dynamics mode (Lamarque et al., 2012) using offline meteorological fields  
4 instead of an online calculation, to allow direct comparisons between different simulations. This  
5 offline meteorology consists of a high frequency meteorological input from a previous free  
6 running climatic simulation.

7 It should be noted that during nighttime the uptake on aerosols of emitted species such as I<sub>2</sub> and  
8 HOI, and the uptake of reservoir species such as IONO<sub>2</sub>, can play a major role in the cycling of  
9 iodine. Observations at CVAO show that I<sub>2</sub> peaked at about 1 pmol/mol during the night and that  
10 ICl was not detected above the 1 pmol/mol detection limit of the instrument (Lawler et al.,  
11 2014). In order to match these observations, we need to reduce the uptake and heterogeneous  
12 recycling of iodine species. The uptake rates of chemical species on the background seasalt  
13 aerosols are determined by their uptake coefficients ( $\gamma$ ). The database of mass accommodation  
14 and/or uptake coefficients is rather sparse and essentially limited to I<sub>2</sub>, HI, HOI, ICI, IBr on pure  
15 water/ice and on sulphuric acid particles (Sander et al., 2006). Other iodine species which are  
16 likely to undergo uptake onto aerosol are OIO, HIO<sub>3</sub>, IONO<sub>2</sub>, IONO<sub>2</sub>, I<sub>2</sub>O<sub>2</sub> (Saiz-Lopez et al.,  
17 2012a; Sommariva et al., 2012). Uptake of HOI is very uncertain, with  $\gamma$ (HOI) ranging from  $2 \times$   
18  $10^{-3}$  to 0.3 depending on the surface composition and state (Holmes et al., 2001). Sommariva et  
19 al. (2012) assumed  $\gamma$ (HOI) to be 0.6, similar to the value for HOBr measured by Wachsmuth et  
20 al. (2002). In the case of IONO<sub>2</sub>, the uptake coefficient has not been measured, with most models  
21 using values of 0.1 (von Glasow et al., 2002; Saiz-Lopez et al., 2008; Mahajan et al., 2009; Leigh  
22 et al., 2010; Mahajan et al., 2010a; Mahajan et al., 2010b; Sommariva et al., 2012; Lawler et al.,  
23 2014). The modelled levels of I<sub>2</sub> and ICl change with different values of uptake coefficients. To

1 match the CVAO I<sub>2</sub> and ICl observations (Lawler et al., 2014), we have used  $\gamma = 0.01$  for HOI  
2 and IONO<sub>2</sub>, which is within the uncertainty in the literature, and assumed that 80% is recycled as  
3 I<sub>2</sub>. Further measurements of these dihalogen species are needed to better constrain their  
4 heterogeneous recycling on seasalt aerosols.

5

## 6 **5. Results and discussion**

7 Of the possible nocturnal iodine activation reactions involving the inorganic iodine source gases  
8 I<sub>2</sub> and HOI, only reactions R1 and R4 appear to be likely candidates (see Section 3). We  
9 therefore designed two modelling scenarios: Scenario 1 (S1), without nighttime reactions of I<sub>2</sub> or  
10 HOI with NO<sub>3</sub>; and Scenario 2 (S2), including reactions R1 and R4 for the degradation of HOI  
11 and I<sub>2</sub> by NO<sub>3</sub>. In the one-dimensional model THAMO, the I<sub>2</sub> and HOI are injected into the  
12 atmosphere from the ocean surface using the flux parameterizations derived from laboratory  
13 experiments (Carpenter et al., 2013; MacDonald et al., 2014). Figure 4 shows the resulting  
14 diurnal evolution of the HOI and I<sub>2</sub> mixing ratios in the two scenarios, after two days of  
15 simulation time. The I<sub>2</sub> mixing ratio peaks during the night in both the scenarios due to quick  
16 loss by photolysis during the daytime. By contrast, HOI is present during daytime due to its  
17 production through the reaction of IO with HO<sub>2</sub>, and peaks just before sunset. In the first  
18 scenario, without the inclusion of reactions R1 and R4, Figure 4 (right-hand side panels) shows  
19 that I<sub>2</sub> builds up during the night, reaching a concentration peak just before dawn. This is  
20 especially noticeable as the daytime concentrations are much lower than during the night. On the  
21 other hand, HOI concentrations decrease during night until dawn, when they drop to zero. For  
22 both species, inclusion of reactions with NO<sub>3</sub> causes a decrease in their respective nocturnal

1 concentrations (Fig. 4, left-hand side panels). The inclusion of reactions R1 and R4 also leads to  
2 a modelled  $I_2$  concentration which is in better agreement with the observations of the molecule  
3 made at CVAO (Lawler et al., 2014), reaching peak values of about 1 pmol/mol, as compared to  
4 about 3 pmol/mol for the scenario without nighttime reactions. An additional consequence of  
5 including reactions R1 and R4 is the significant increase of the sea-air fluxes of HOI and  $I_2$  at  
6 night due to their atmospheric removal by  $NO_3$  (Fig. 4, bottom panel).

7 Figure 5 shows the diurnal evolution of IO,  $NO_3$  and  $IONO_2$  in both model scenarios after two  
8 days of simulation time. Although the daytime peak values of IO are well reproduced in both  
9 scenarios, reaching about 1.5 pmol/mol around noon similar to the ground-based observations  
10 (Read et al., 2008), the inclusion of reactions R1 and R4 leads to the removal of the dawn spike  
11 in IO, which is predicted by current iodine models but was not observed at CVAO (Read et al.,  
12 2008; Mahajan et al., 2010a). The IO dawn spike predicted by models is due to a buildup of the  
13 emitted  $I_2$  and HOI (which is converted into IBr/ICl through heterogeneous recycling) over the  
14 night, followed by rapid photolysis after first sunlight. However, due to the considerable removal  
15 of HOI and  $I_2$  through the night due to reaction with ambient  $NO_3$ , this spike does not appear in  
16 the second scenario, leading to a modification of the diurnal profile of IO that better matches  
17 with observations.

18 Reactions R1 and R4 also reduce the  $NO_3$  mixing ratio (Fig. 5, middle panels). In scenario 1, the  
19  $NO_3$  is modelled to peak at about 14 pmol/mol just before dawn. However, the inclusion of  
20 reactions R1 and R4 leads to near complete depletion of  $NO_3$  close to the surface, with the peak  
21 level at the surface reaching only 2 pmol/mol, since reactions R1 and R4 become the main  
22 atmospheric loss processes for  $NO_3$  in the lower MBL. These reactions lead however to the  
23 buildup of  $IONO_2$  during the night (Fig. 5, bottom panels). In the absence of reactions R1 and

1 R4, significant levels of IONO<sub>2</sub> are seen only at dawn and dusk since no other reactions produce  
2 IONO<sub>2</sub> at night, and during the day IONO<sub>2</sub> is removed by photolysis. However, with continuous  
3 conversion of I<sub>2</sub> and HOI to IONO<sub>2</sub> by reactions R1 and R4 in scenario 2, IONO<sub>2</sub> is modelled to  
4 reach up to 3 pmol/mol in the nocturnal MBL.

5 Given the associated uncertainty in the theoretical estimate of the  $k_4$ , we used THAMO to assess  
6 the sensitivity of surface NO<sub>3</sub> to  $k_4$ . Figure 6 shows that NO<sub>3</sub> peak nighttime concentration is in  
7 fact highly coupled to  $k_4$ , with the expected uncertainty in  $k_4$  of one order of magnitude (see  
8 above) giving rise to a factor of two change in NO<sub>3</sub>. A laboratory measurement of  $k_4$  should  
9 therefore be undertaken in the future.

10 We now implement the nighttime reactions in the 3D global model (CAM-Chem) to assess the  
11 resulting geographical distributions and impacts of these reactions. We have also run two  
12 different scenarios in CAM-Chem, the first without R1 and R4 in the chemical scheme, and the  
13 second including the new nighttime iodine chemistry. Figure 7 shows how the inclusion of R1  
14 and R4 reduces globally the nighttime concentrations of I<sub>2</sub> and HOI. The plots correspond to the  
15 nighttime averaged (from 00LT to 01LT (Local Time)) differences between the model scenarios.  
16 Considerable reductions of up to 0.5 and 10 pmol/mol (i.e. up to 100% removal) are observed for  
17 I<sub>2</sub> and HOI, respectively, particularly over coastal polluted regions where continental pollution  
18 outflow leads to higher levels of NO<sub>3</sub> in the nighttime MBL. Major shipping routes also show  
19 strong nocturnal iodine activity due to the characteristically high NO<sub>x</sub>, and resulting NO<sub>3</sub>,  
20 associated with shipping emissions.

21 Figure 8 shows the effect of this nocturnal chemistry on the concentrations of IONO<sub>2</sub> and NO<sub>3</sub>.  
22 As in the previous figure, the plots correspond to the nighttime averaged difference between the

1 second and the first scenarios. The maps show an increase of IONO<sub>2</sub> of up to 15 pmol/mol  
2 (~600%) over polluted coastal areas, due to efficient conversion of NO<sub>3</sub> into IONO<sub>2</sub>. The bottom  
3 panel of Figure 7 shows the expected decrease of NO<sub>3</sub> levels associated with the inclusion of  
4 reactions R1 and R4, with decreases of up to ~4 pmol/mol (up to 60%) over marine polluted  
5 regions. We model global percentage reductions in the NO<sub>3</sub> concentrations of 7.1% (60S-60N),  
6 with nitrate removal of up to 80% in non-polluted remote oceanic regions with low NO<sub>3</sub> levels.  
7 This in turn can affect the modelled oxidation of DMS by NO<sub>3</sub>. We estimate that the reduction in  
8 NO<sub>3</sub>, due to the inclusion of R1 and R4, results in a model increase in DMS levels of up to 7  
9 pmol/mol (about 20%) in marine regions affected by continental pollution outflow (Fig. 9). We  
10 therefore suggest that the inclusion of the new nighttime iodine chemistry can have a large, so far  
11 unrecognized, impact on the nocturnal oxidizing capacity of the marine atmosphere.

12 The hourly evolution of the main species involved in this study is shown in Figures 10 and 11,  
13 which include the levels of HOI, I<sub>2</sub>, IONO<sub>2</sub> and NO<sub>3</sub> in the MBL over regions where nocturnal  
14 iodine is modelled to be particularly active. The first region is located within the Mediterranean  
15 Sea, an area that shows large differences during the summer months when high ozone levels  
16 drive large emissions of HOI and I<sub>2</sub> from the sea, and the high levels of NO<sub>3</sub> at nighttime make  
17 this chemistry especially important. The hourly average in August is shown in Figure 10 for  
18 HOI, IONO<sub>2</sub> and I<sub>2</sub>. HOI and IONO<sub>2</sub> (Fig 10 ) are the species whose concentration differ most  
19 between scenarios as HOI is removed and IONO<sub>2</sub> produced by R4 (and, to a lesser extent, R1).  
20 Over a Pacific Ocean region at the south of the Baja California Peninsula, the modelled  
21 differences between the two scenarios are even higher than over the Mediterranean Sea (Figure  
22 11). Large differences in MBL NO<sub>3</sub>, up to 28%, are modelled during the night caused by  
23 pollution outflow from the west coasts of Mexico and USA.



1

## 2 **6. Summary and conclusions**

3 The viability of the reaction of HOI with NO<sub>2</sub>, HNO<sub>3</sub> and NO<sub>3</sub> has been studied by theoretical  
4 calculations. The results indicate that only the reaction of HOI with NO<sub>3</sub>, to yield IO + HNO<sub>3</sub>, is  
5 possible under tropospheric conditions. The inclusion of this reaction, along with that of I<sub>2</sub> +  
6 NO<sub>3</sub>, has a number of significant implications: *i*) nocturnal iodine radical chemistry is activated;  
7 *ii*) this causes enhanced nighttime oceanic emissions of HOI and I<sub>2</sub>; *iii*) nighttime iodine species  
8 are partitioned into high levels of IONO<sub>2</sub>; *iv*) the IO spike, modelled by current iodine models  
9 but not shown by observations, is removed; and, *v*) a reduction of the levels of nitrate radical in  
10 the MBL, with the associated less efficient oxidation of DMS, which has important implications  
11 for our understanding of the nocturnal oxidizing capacity of the marine atmosphere.

12

13

## 14 **Acknowledgments**

15 This work was supported by the Spanish National Research Council (CSIC). The National  
16 Center for Atmospheric Research (NCAR) is funded by the National Science Foundation NSF.  
17 The Climate Simulation Laboratory at NCAR's Computational and Information Systems  
18 Laboratory (CISL) provided the computing resources (ark:/85065/d7wd3xhc). As part of the  
19 CESM project, CAM-Chem is supported by the NSF and the Office of Science (BER) of the US  
20 Department of Energy. This work was also sponsored by the NASA Atmospheric Composition  
21 Modeling and Analysis Program Activities (ACMAP, number NNX11AH90G).

1

## 2 **References**

3 Allan, B. J., McFiggans, G., Plane, J. M. C., Coe, H., and McFadyen, G. G.: The nitrate radical  
4 in the remote marine boundary layer, *Journal of Geophysical Research: Atmospheres*, 105,  
5 24191-24204, 10.1029/2000jd900314, 2000.

6 Allan, J. D., Williams, P. I., Najera, J., Whitehead, J. D., Flynn, M. J., Taylor, J. W., Liu, D.,  
7 Darbyshire, E., Carpenter, L. J., Chance, R., Andrews, S. J., Hackenberg, S. C., and McFiggans,  
8 G.: Iodine observed in new particle formation events in the Arctic atmosphere during  
9 ACCACIA, *Atmos. Chem. Phys.*, 15, 5599-5609, 10.5194/acp-15-5599-2015, 2015.

10 Bartis, J. T., and Widom, B.: Stochastic models of the interconversion of three or more chemical  
11 species, *J. Chem. Phys.*, 60, 3474-3482, doi: 10.1063/1.1681562, 1974.

12 Butler, J. H., King, D. B., Lobert, J. M., Montzka, S. A., Yvon-Lewis, S. A., Hall, B. D.,  
13 Warwick, N. J., Mondeel, D. J., Aydin, M., and Elkins, J. W.: Oceanic distributions and  
14 emissions of short-lived halocarbons, *Global Biogeochem. Cycles*, 21, GB1023,  
15 10.1029/2006gb002732, 2007.

16 Carpenter, L. J.: Iodine In the marine Boundary Layer, *Chem. Rev.*, 103 (12), 4953-4962, 2003.

17 Carpenter, L. J., Fleming, Z. L., Read, K. A., Lee, J. D., Moller, S. J., Hopkins, J. R., Purvis, R.  
18 M., Lewis, A. C., Müller, K., Heinold, B., Herrmann, H., Fomba, K. W., Pinxteren, D., Müller,  
19 C., Tegen, I., Wiedensohler, A., Müller, T., Niedermeier, N., Achterberg, E. P., Patey, M. D.,  
20 Kozlova, E. A., Heimann, M., Heard, D. E., Plane, J. M. C., Mahajan, A., Oetjen, H., Ingham, T.,  
21 Stone, D., Whalley, L. K., Evans, M. J., Pilling, M. J., Leigh, R. J., Monks, P. S., Karunaharan,

1 A., Vaughan, S., Arnold, S. R., Tschirner, J., Pöhler, D., Frieß, U., Holla, R., Mendes, L. M.,  
2 Lopez, H., Faria, B., Manning, A. J., and Wallace, D. W. R.: Seasonal characteristics of tropical  
3 marine boundary layer air measured at the Cape Verde Atmospheric Observatory, *J. Atmos.*  
4 *Chem.*, 67, 87-140, 10.1007/s10874-011-9206-1, 2011.

5 Carpenter, L. J., MacDonald, S. M., Shaw, M. D., Kumar, R., Saunders, R. W., Parthipan, R.,  
6 Wilson, J., and Plane, J. M. C.: Atmospheric iodine levels influenced by sea surface emissions of  
7 inorganic iodine, *Nature Geosci.*, 6, 108-111, 10.1038/ngeo1687, 2013.

8 Carpenter, L. J., Andrews, S. J., Lidster, R. T., Saiz-Lopez, A., Fernandez-Sanchez, M., Bloss,  
9 W. J., Ouyang, B., and Jones, R. L.: A nocturnal atmospheric loss of CH<sub>2</sub>I<sub>2</sub> in the remote marine  
10 boundary layer, *J. Atmos. Chem.*, 10.1007/s10874-015-9320-6, 2015.

11 Fernandez, R. P., Salawitch, R. J., Kinnison, D. E., Lamarque, J. F., and Saiz-Lopez, A.:  
12 Bromine partitioning in the tropical tropopause layer: implications for stratospheric injection,  
13 *Atmos. Chem. Phys.*, 14, 13391-13410, 10.5194/acp-14-13391-2014, 2014.

14 Frisch, M., Trucks, G., Schlegel, H., Scuseria, G., Robb, M., Cheeseman, J., Scalmani, G.,  
15 Barone, V., Mennucci, B., and Petersson, G.: Gaussian 09, Revision A. 1. Wallingford, CT:  
16 Gaussian, Inc, 2009.

17 Georgievskii, Y., and Klippenstein, S. J.: Long-range transition state theory, *J. Chem. Phys.*, 122,  
18 194103, doi: 10.1063/1.1899603, 2005.

19 Gilbert, R. G., and Smith, S. C.: *Theory of Unimolecular and Recombination Reactions*,  
20 Blackwell, Oxford, 1990.

1 Glukhovtsev, M. N., Pross, A., McGrath, M. P., and Radom, L.: Extension of Gaussian-2 (G2)  
2 theory to bromine- and iodine-containing molecules: Use of effective core potentials, *J. Chem.*  
3 *Phys.*, 103, 1878-1885, 1995.

4 Gomez Martin, J. C., Galvez, O., Baeza-Romero, M. T., Ingham, T., Plane, J. M. C., and Blitz,  
5 M. A.: On the mechanism of iodine oxide particle formation, *Phys. Chem. Chem. Phys.*, 15,  
6 15612-15622, 10.1039/c3cp51217g, 2013.

7 Gómez Martín, J. C., Mahajan, A. S., Hay, T. D., Prados-Román, C., Ordóñez, C., MacDonald,  
8 S. M., Plane, J. M. C., Sorribas, M., Gil, M., Paredes Mora, J. F., Agama Reyes, M. V., Oram, D.  
9 E., Leedham, E., and Saiz-Lopez, A.: Iodine chemistry in the eastern Pacific marine boundary  
10 layer, *Journal of Geophysical Research: Atmospheres*, 118, 887-904, 10.1002/jgrd.50132, 2013.

11 Großmann, K., Frieß, U., Peters, E., Wittrock, F., Lampel, J., Yilmaz, S., Tschritter, J.,  
12 Sommariva, R., von Glasow, R., Quack, B., Krüger, K., Pfeilsticker, K., and Platt, U.: Iodine  
13 monoxide in the Western Pacific marine boundary layer, *Atmos. Chem. Phys.*, 13, 3363-3378,  
14 10.5194/acp-13-3363-2013, 2013.

15 Hoffmann, T., O'Dowd, C. D., and Seinfeld, J. H.: Iodine oxide homogeneous nucleation: An  
16 explanation for coastal new particle production, *Geophys. Res. Lett.*, 28, 1949-1952, 2001.

17 Holmes, N. S., Adams, J. W., and Crowley, J. N.: Uptake and reaction of HOI and IONO<sub>2</sub> on  
18 frozen and dry NaCl/NaBr surfaces and H<sub>2</sub>SO<sub>4</sub>, *Phys. Chem. Chem. Phys.*, 3, 1679-1687,  
19 10.1039/b100247n, 2001.

- 1 Jones, C. E., Hornsby, K. E., Sommariva, R., Dunk, R. M., von Glasow, R., McFiggans, G., and  
2 Carpenter, L. J.: Quantifying the contribution of marine organic gases to atmospheric iodine,  
3 *Geophys. Res. Lett.*, 37, L18804, 2010.
- 4 Kaltsoyannis, N., and Plane, J. M. C.: Quantum chemical calculations on a selection of iodine-  
5 containing species (IO, OIO,  $\text{INO}_3$ ,  $(\text{IO})_2$ ,  $\text{I}_2\text{O}_3$ ,  $\text{I}_2\text{O}_4$  and  $\text{I}_2\text{O}_5$ ) of importance in the atmosphere.,  
6 *Phys. Chem. Chem. Phys.*, 10, 1723-1733, 2008.
- 7 Khanniche, S., Louis, F., Cantrel, L., and Černušák, I.: A Density Functional Theory and ab  
8 Initio Investigation of the Oxidation Reaction of CO by IO Radicals, *J. Phys. Chem. A*, 120,  
9 1737–1749, 2016.
- 10 Lamarque, J. F., Emmons, L. K., Hess, P. G., Kinnison, D. E., Tilmes, S., Vitt, F., Heald, C. L.,  
11 Holland, E. A., Lauritzen, P. H., Neu, J., Orlando, J. J., Rasch, P. J., and Tyndall, G. K.: CAM-  
12 chem: description and evaluation of interactive atmospheric chemistry in the Community Earth  
13 System Model, *Geosci. Model Dev.*, 5, 369-411, 10.5194/gmd-5-369-2012, 2012.
- 14 Lawler, M. J., Mahajan, A. S., Saiz-Lopez, A., and Saltzman, E. S.: Observations of  $\text{I}_2$  at a  
15 remote marine site, *Atmos. Chem. Phys.*, 14, 2669-2678, 10.5194/acp-14-2669-2014, 2014.
- 16 Lee, J. D., Moller, S. J., Read, K. A., Lewis, A. C., Mendes, L., and Carpenter, L. J.: Year-round  
17 measurements of nitrogen oxides and ozone in the tropical North Atlantic marine boundary layer,  
18 *Journal of Geophysical Research: Atmospheres*, 114, n/a-n/a, 10.1029/2009jd011878, 2009.
- 19 Lee, J. D., McFiggans, G., Allan, J. D., Baker, A. R., Ball, S. M., Benton, A. K., Carpenter, L. J.,  
20 Commane, R., Finley, B. D., Evans, M., Fuentes, E., Furneaux, K., Goddard, A., Good, N.,  
21 Hamilton, J. F., Heard, D. E., Herrmann, H., Hollingsworth, A., Hopkins, J. R., Ingham, T.,

1 Irwin, M., Jones, C. E., Jones, R. L., Keene, W. C., Lawler, M. J., Lehmann, S., Lewis, A. C.,  
2 Long, M. S., Mahajan, A., Methven, J., Moller, S. J., Müller, K., Müller, T., Niedermeier, N.,  
3 O'Doherty, S., Oetjen, H., Plane, J. M. C., Pszenny, A. A. P., Read, K. A., Saiz-Lopez, A.,  
4 Saltzman, E. S., Sander, R., von Glasow, R., Whalley, L., Wiedensohler, A., and Young, D.:  
5 Reactive Halogens in the Marine Boundary Layer (RHAMBLe): the tropical North Atlantic  
6 experiments, *Atmos. Chem. Phys.*, 10, 1031-1055, 10.5194/acp-10-1031-2010, 2010.

7 Leigh, R. J., Ball, S. M., Whitehead, J., Leblanc, C., Shillings, A. J. L., Mahajan, A. S., Oetjen,  
8 H., Dorsey, J. R., Gallagher, M., Jones, R. L., Plane, J. M. C., Potin, P., and McFiggans, G.:  
9 Measurements and modelling of molecular iodine emissions, transport and photodestruction in  
10 the coastal region around Roscoff, *Atmos. Chem. Phys.*, 10, 11823-11838, 2010.

11 MacDonald, S. M., Gómez Martín, J. C., Chance, R., Warriner, S., Saiz-Lopez, A., Carpenter, L.  
12 J., and Plane, J. M. C.: A laboratory characterisation of inorganic iodine emissions from the sea  
13 surface: dependence on oceanic variables and parameterisation for global modelling, *Atmos.*  
14 *Chem. Phys.*, 14, 5841-5852, 10.5194/acp-14-5841-2014, 2014.

15 Mahajan, A. S., Oetjen, H., Saiz-Lopez, A., Lee, J. D., McFiggans, G. B., and Plane, J. M. C.:  
16 Reactive iodine species in a semi-polluted environment, *Geophys. Res. Lett.*, 36, L16803,  
17 doi:16810.11029/12009GL038018, 2009.

18 Mahajan, A. S., Plane, J. M. C., Oetjen, H., Mendes, L., Saunders, R. W., Saiz-Lopez, A., Jones,  
19 C. E., Carpenter, L. J., and McFiggans, G. B.: Measurement and modelling of tropospheric  
20 reactive halogen species over the tropical Atlantic Ocean, *Atmos. Chem. Phys.*, 10, 4611-4624,  
21 2010a.

1 Mahajan, A. S., Shaw, M., Oetjen, H., Hornsby, K. E., Carpenter, L. J., Kaleschke, L., Tian-  
2 Kunze, X., Lee, J. D., Moller, S. J., Edwards, P., Commane, R., Ingham, T., Heard, D. E., and  
3 Plane, J. M. C.: Evidence of reactive iodine chemistry in the Arctic boundary layer, *J. Geophys.*  
4 *Res.*, [Atmos.], 115, D20303, doi:10.1029/2009JD013665, 2010b.

5 Mahajan, A. S., Gómez Martín, J. C., Hay, T. D., Royer, S. J., Yvon-Lewis, S., Liu, Y., Hu, L.,  
6 Prados-Roman, C., Ordóñez, C., Plane, J. M. C., and Saiz-Lopez, A.: Latitudinal distribution of  
7 reactive iodine in the Eastern Pacific and its link to open ocean sources, *Atmos. Chem. Phys.*, 12,  
8 11609-11617, 10.5194/acp-12-11609-2012, 2012.

9 McFiggans, G., Coe, H., Burgess, R., Allan, J., Cubison, M., Alfarra, M. R., Saunders, R., Saiz-  
10 Lopez, A., Plane, J. M. C., Wevill, D. J., Carpenter, L. J., Rickard, A. R., and Monks, P. S.:  
11 Direct evidence for coastal iodine particles from *Laminaria* macroalgae - linkage to emissions of  
12 molecular iodine, *Atmos. Chem. Phys.*, 4, 701-713, 2004.

13 Mečiarová, K., Šulka, M., Canneaux, S., Louis, F., and Černušáka, I.: A theoretical study of the  
14 kinetics of the forward and reverse reactions  $\text{HI} + \text{CH}_3 = \text{I} + \text{CH}_4$ , *Chem. Phys. Lett.*, 517, 149-  
15 154, 2011.

16 Nakano, Y., Ukeguchi, H., and Ishiwata, T.: Rate constant of the reaction of  $\text{NO}_3$  with  $\text{CH}_2\text{I}_2$   
17 measured with use of cavity ring-down spectroscopy, *Chem. Phys. Lett.*, 430, 235-239, doi:  
18 10.1016/j.cplett.2006.09.002, 2006.

19 O'Dowd, C. D., Jimenez, J. L., Bahreini, R., Flagan, R. C., Seinfeld, J. H., Hameri, K., Pirjola,  
20 L., Kulmala, M., Jennings, S. G., and Hoffmann, T.: Marine aerosol formation from biogenic  
21 iodine emissions, *Nature*, 417, 632-636, 2002.

1 Ordóñez, C., Lamarque, J. F., Tilmes, S., Kinnison, D. E., Atlas, E. L., Blake, D. R., Sousa  
2 Santos, G., Brasseur, G., and Saiz-Lopez, A.: Bromine and iodine chemistry in a global  
3 chemistry-climate model: description and evaluation of very short-lived oceanic sources, *Atmos.*  
4 *Chem. Phys.*, 12, 1423-1447, 10.5194/acp-12-1423-2012, 2012.

5 Prados-Roman, C., Cuevas, C. A., Fernandez, R. P., Kinnison, D. E., Lamarque, J. F., and Saiz-  
6 Lopez, A.: A negative feedback between anthropogenic ozone pollution and enhanced ocean  
7 emissions of iodine, *Atmos. Chem. Phys.*, 15, 2215-2224, 10.5194/acp-15-2215-2015, 2015a.

8 Prados-Roman, C., Cuevas, C. A., Hay, T., Fernandez, R. P., Mahajan, A. S., Royer, S. J., Galí,  
9 M., Simó, R., Dachs, J., Großmann, K., Kinnison, D. E., Lamarque, J. F., and Saiz-Lopez, A.:  
10 Iodine oxide in the global marine boundary layer, *Atmos. Chem. Phys.*, 15, 583-593,  
11 10.5194/acp-15-583-2015, 2015b.

12 Read, K. A., Mahajan, A. S., Carpenter, L. J., Evans, M. J., Faria, B. V. E., Heard, D. E.,  
13 Hopkins, J. R., Lee, J. D., Moller, S. J., Lewis, A. C., Mendes, L., McQuaid, J. B., Oetjen, H.,  
14 Saiz-Lopez, A., Pilling, M. J., and Plane, J. M. C.: Extensive halogen-mediated ozone  
15 destruction over the tropical Atlantic Ocean, *Nature*, 453, 1232-1235, 2008.

16 Read, K. A., Lee, J. D., Lewis, A. C., Moller, S. J., Mendes, L., and Carpenter, L. J.: Intra-annual  
17 cycles of NMVOC in the tropical marine boundary layer and their use for interpreting seasonal  
18 variability in CO, *Journal of Geophysical Research: Atmospheres*, 114, n/a-n/a,  
19 10.1029/2009jd011879, 2009.

20 Roberston, S. H., Glowacki, D. R., Liang, C. H., Morley, C., Shannon, R., Blitz, M., and Pilling,  
21 M. J.: MESMER (Master Equation Solver for Multi-Energy Well Reactions), 2008–2012: An



1 object oriented C++ program for carrying out ME calculations and eigenvalue-eigenvector  
2 analysis on arbitrary multiple well systems, edited. [Available at  
3 <http://sourceforge.net/projects/mesmer>.], in, 4.1 ed., 2014.

4 Roscoe, H. K., Jones, A. E., Brough, N., Weller, R., Saiz-Lopez, A., Mahajan, A. S.,  
5 Schoenhardt, A., Burrows, J. P., and Fleming, Z. L.: Particles and iodine compounds in coastal  
6 Antarctica, *Journal of Geophysical Research: Atmospheres*, 120, 7144-7156,  
7 10.1002/2015jd023301, 2015.

8 Saiz-Lopez, A., and Plane, J. M. C.: Novel iodine chemistry in the marine boundary layer,  
9 *Geophys. Res. Lett.*, 31, L04112, 2004.

10 Saiz-Lopez, A., Plane, J. M. C., Mahajan, A. S., Anderson, P. S., Bauguitte, S. J.-B., Jones, A.  
11 E., Roscoe, H. K., Salmon, R. A., Bloss, W. J., Lee, J. D., and Heard, D. E.: On the vertical  
12 distribution of boundary layer halogens over coastal Antarctica: implications for O<sub>3</sub>, HO<sub>x</sub>, NO<sub>x</sub>  
13 and the Hg lifetime, *Atmos. Chem. Phys.*, 8, 887-900, 2008.

14 Saiz-Lopez, A., Lamarque, J.-F., Kinnison, D., Tilmes, S., Ordóñez, C., Orlando, J. J., Conley,  
15 A. J., Plane, J. M. C., Mahajan, A., Sousa Santos, G., Atlas, E., Blake, D. R., Sander, S. P.,  
16 Schauffler, S. M., Thompson, A. M., and Brasseur, G.: Estimating the climate significance of  
17 halogen-driven ozone loss in the tropical marine troposphere, *Atmos. Chem. Phys.*, 12, 3939-  
18 3949, 2012a.

19 Saiz-Lopez, A., Plane, J. M. C., Baker, A. R., Carpenter, L. J., Von Glasow, R., Gómez Martín,  
20 J. C., McFiggans, G., and Saunders, R. W.: Atmospheric Chemistry of Iodine, *Chem. Rev.*  
21 (Washington, DC, U. S.), 112, 1773-1804, 10.1021/cr200029u, 2012b.

1 Saiz-Lopez, A., Fernandez, R. P., Ordóñez, C., Kinnison, D. E., Gómez Martín, J. C., Lamarque,  
2 J. F., and Tilmes, S.: Iodine chemistry in the troposphere and its effect on ozone, *Atmos. Chem.*  
3 *Phys.*, 14, 13119-13143, 10.5194/acp-14-13119-2014, 2014.

4 Saiz-Lopez, A., Baidar, S., Cuevas, C. A., Koenig, T. K., Fernandez, R. P., Dix, B., Kinnison, D.  
5 E., Lamarque, J. F., Rodriguez-Lloveras, X., Campos, T. L., and Volkamer, R.: Injection of  
6 iodine to the stratosphere, *Geophys. Res. Lett.*, n/a-n/a, 10.1002/2015gl064796, 2015.

7 Sander, S. P., Orkin, V. L., Kurylo, M. J., Golden, D. M., Huie, R. E., Kolb, C. E., Finlayson-  
8 Pitts, B. J., Molina, M. J., Friedl, R. R., Ravishankara, A. R., Moortgat, G. K., Keller-Rudek, H.,  
9 and Wine, P. H.: Chemical kinetics and photochemical data for use in atmospheric studies, JPL-  
10 NASA, 2006.

11 Sherwen, T., Evans, M. J., Carpenter, L. J., Andrews, S. J., Lidster, R. T., Dix, B., Koenig, T. K.,  
12 Sinreich, R., Ortega, I., Volkamer, R., Saiz-Lopez, A., Prados-Roman, C., Mahajan, A. S., and  
13 Ordóñez, C.: Iodine's impact on tropospheric oxidants: a global model study in GEOS-Chem,  
14 *Atmos. Chem. Phys.*, 16, 1161-1186, 10.5194/acp-16-1161-2016, 2016.

15 Simpson, W. R., Brown, S. S., Saiz-Lopez, A., Thornton, J. A., and Glasow, R. v.: Tropospheric  
16 Halogen Chemistry: Sources, Cycling, and Impacts, *Chem. Rev.*, 115, 4035-4062,  
17 10.1021/cr5006638, 2015.

18 Sommariva, R., Bloss, W. J., and von Glasow, R.: Uncertainties in gas-phase atmospheric iodine  
19 chemistry, *Atmos. Environ.*, 57, 219-232, doi: 10.1016/j.atmosenv.2012.04.032, 2012.

1 Šulková, K., Šulka, M., Louis, F., and Neogrady, P.: Atmospheric Reactivity of CH<sub>2</sub>ICl with OH  
2 Radicals: High-Level OVOS CCSD(T) Calculations for the X-Abstraction Pathways (X = H, Cl,  
3 or I), *J. Phys. Chem. A*, 117, 771–782, 2013.

4 Volkamer, R., Baidar, S., Campos, T. L., Coburn, S., DiGangi, J. P., Dix, B., Eloranta, E. W.,  
5 Koenig, T. K., Morley, B., Ortega, I., Pierce, B. R., Reeves, M., Sinreich, R., Wang, S., Zondlo,  
6 M. A., and Romashkin, P. A.: Aircraft measurements of BrO, IO, glyoxal, NO<sub>2</sub>, H<sub>2</sub>O, O<sub>2</sub>–O<sub>2</sub>  
7 and aerosol extinction profiles in the tropics: comparison with aircraft-/ship-based in situ and  
8 lidar measurements, *Atmos. Meas. Tech.*, 8, 2121-2148, 10.5194/amt-8-2121-2015, 2015.

9 von Glasow, R., Sander, R., Bott, A., and Crutzen, P. J.: Modeling halogen chemistry in the  
10 marine boundary layer. 1. Cloud-free MBL, *J. Geophys. Res.*, 107, 4341, 2002.

11 Wachsmuth, M., Gäggeler, H. W., von Glasow, R., and Ammann, M.: Accommodation  
12 coefficient of HOBr on deliquescent sodium bromide aerosol particles, *Atmos. Chem. Phys.*, 2,  
13 121-131, 10.5194/acp-2-121-2002, 2002.

14 Wang, F., Saiz-Lopez, A., Mahajan, A. S., Gómez Martín, J. C., Armstrong, D., Lemes, M., Hay,  
15 T., and Prados-Roman, C.: Enhanced production of oxidised mercury over the tropical Pacific  
16 Ocean: a key missing oxidation pathway, *Atmos. Chem. Phys.*, 14, 1323-1335, 10.5194/acp-14-  
17 1323-2014, 2014.

18

19

1 **Tables**

2

3 Table 1: Night time reactions of emitted inorganic iodine compounds considered in addition to  
 4 the iodine chemistry scheme used by (Saiz-Lopez et al., 2014).

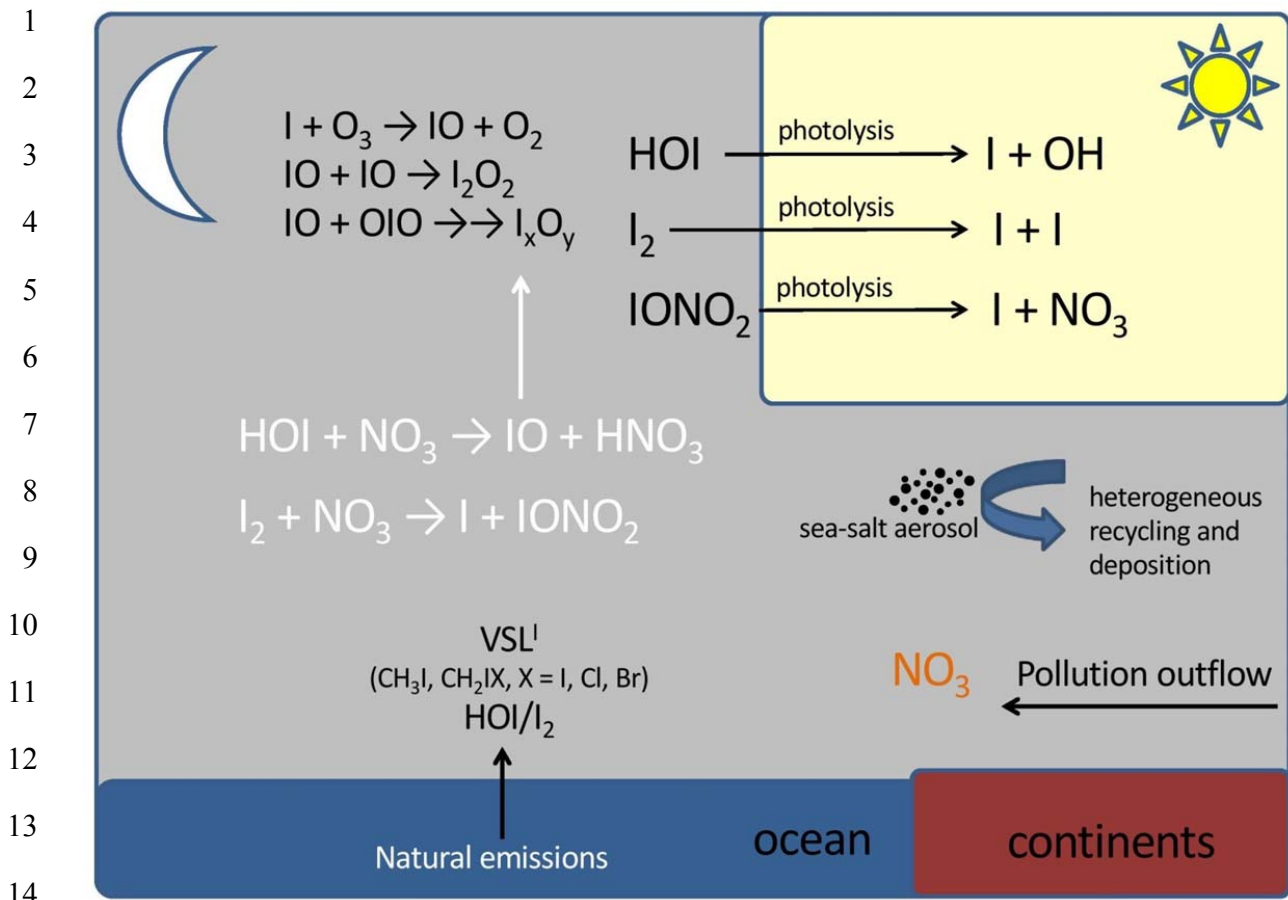
No.	Reaction	Notes
R1.	$I_2 + NO_3 \rightarrow I + IONO_2$	$1.5 \times 10^{-12} \text{ cm}^3 \text{ molecule}^{-1} \text{ s}^{-1}$ [ <i>Chambers et al.</i> , 1992]
R2.	$HOI + NO_2 \rightarrow I + HNO_3$	Endothermic by $9 \text{ kJ mol}^{-1}$ and the transition state is $73 \text{ kJ mol}^{-1}$ above the reactants
R3.	$HOI + HNO_3 \rightarrow IONO_2 + H_2O$	Exothermic by $11 \text{ kJ mol}^{-1}$ . The reaction first forms a complex $21 \text{ kJ mol}^{-1}$ below the reactants but this rearranges to the products via a transition state that is $110 \text{ kJ mol}^{-1}$ above the reactants.
R4.	$HOI + NO_3 \rightarrow IO + HNO_3$	Exothermic by $11 \text{ kJ mol}^{-1}$ with all transition states below the reactants.  $k(T) = 2.7 \times 10^{-12} (300 \text{ K} / T)^{2.66} \text{ cm}^3 \text{ molecule}^{-1} \text{ s}^{-1}$

5  
6

1 **Table 2.** Calculated vibrational frequencies, rotational constants and energies of the stationary  
 2 points and asymptotes on the HOI + NO<sub>3</sub> doublet potential energy surface

Species	Geometry <sup>a</sup>	Vibrational frequencies <sup>b</sup>	Rotational constants <sup>c</sup>	Potential energy <sup>d</sup>
HOI + NO <sub>3</sub>		603, 1084, 3803 & 261, 261, 805, 1108, 1108, 1126	623.9, 8.182, 8.076 & 13.84, 13.84, 6.919	0.0
IOH-NO <sub>3</sub> complex	O 1.623, 0.284, -0.331 H 1.484, -0.657, -0.043 I 0.009, 1.205, 0.286 N -0.456, -2.265, 0.030 O -1.052, -3.321, -0.0473 O -1.147, -1.195, -0.228 O 0.742, -2.161, 0.333	55, 84, 118, 161, 196, 615, 629, 667, 705, 803, 968, 1228, 1273, 1491, 3268	5.610, 0.916, 0.806	-24.0
IO-H-NO <sub>2</sub> TS	O 0.309, 1.515, 0.247 H -0.834, 1.314, -0.017 I 1.280, -0.089, -0.093 N -2.349, -0.133, 0.019 O -3.518, -0.429, -0.035 O -1.444, -0.962, 0.257 O -2.019, 1.117, -0.187	1249i, 70, 97, 103, 225, 472, 676, 698, 797, 806, 1041, 1147, 1308, 1513, 1626	6.300, 0.864, 0.767	-16.4
IO-HNO <sub>3</sub> complex	O 0.571, 1.350, 0.348 H -1.111, 1.098, -0.020 I 1.870, 0.0645, -0.152 N -2.503, -0.202, 0.0186 O -3.673, -0.396, -0.170 O -1.654, -0.986, 0.401 O -2.081, 1.090, -0.242	35, 43, 76, 126, 198, 623, 677, 703, 772, 798, 939, 1331, 1416, 1713, 3281	7.058, 0.605, 0.566	-34.8
IO + HNO <sub>3</sub>		648 & 477, 585, 649, 782, 901, 1320, 1345, 1738, 3724	9.844 & 13.01, 12.05, 6.258	-10.6

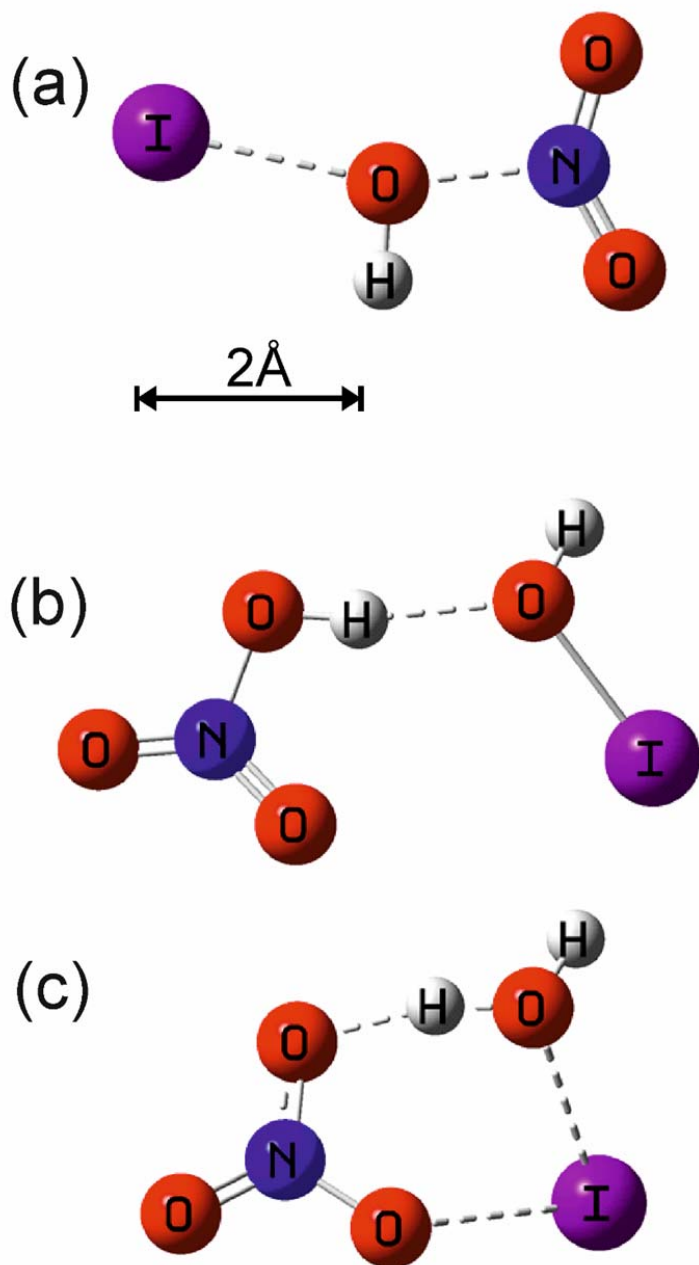
3 <sup>a</sup> Cartesian co-ordinates in Å. <sup>b</sup> **Given as wavenumber** in cm<sup>-1</sup>. <sup>c</sup> In GHz. <sup>d</sup> In kJ mol<sup>-1</sup>, including zero-  
 4 point energy and spin-orbit coupling of I and IO (see text).



15 **Figure 1.** New nocturnal iodine chemistry (in white) implemented in the THAMO and CAM-  
16 Chem models.

17  
18  
19  
20  
21  
22  
23  
24  
25

1



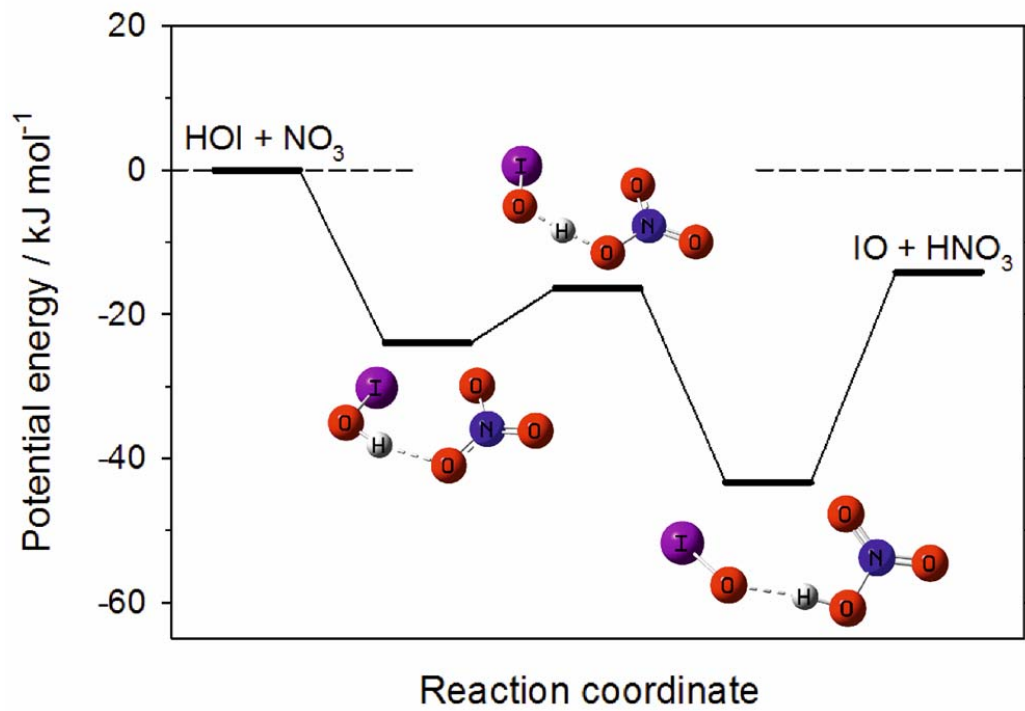
2

3

4

5 **Figure 2:** (a) Transition state for the reaction between HOI and NO<sub>2</sub> to form HNO<sub>3</sub> + I; (b)  
6 complex formed between HOI and HNO<sub>3</sub>, which then reacts via transition state (c) to form  
7 IONO<sub>2</sub> + H<sub>2</sub>O.

1



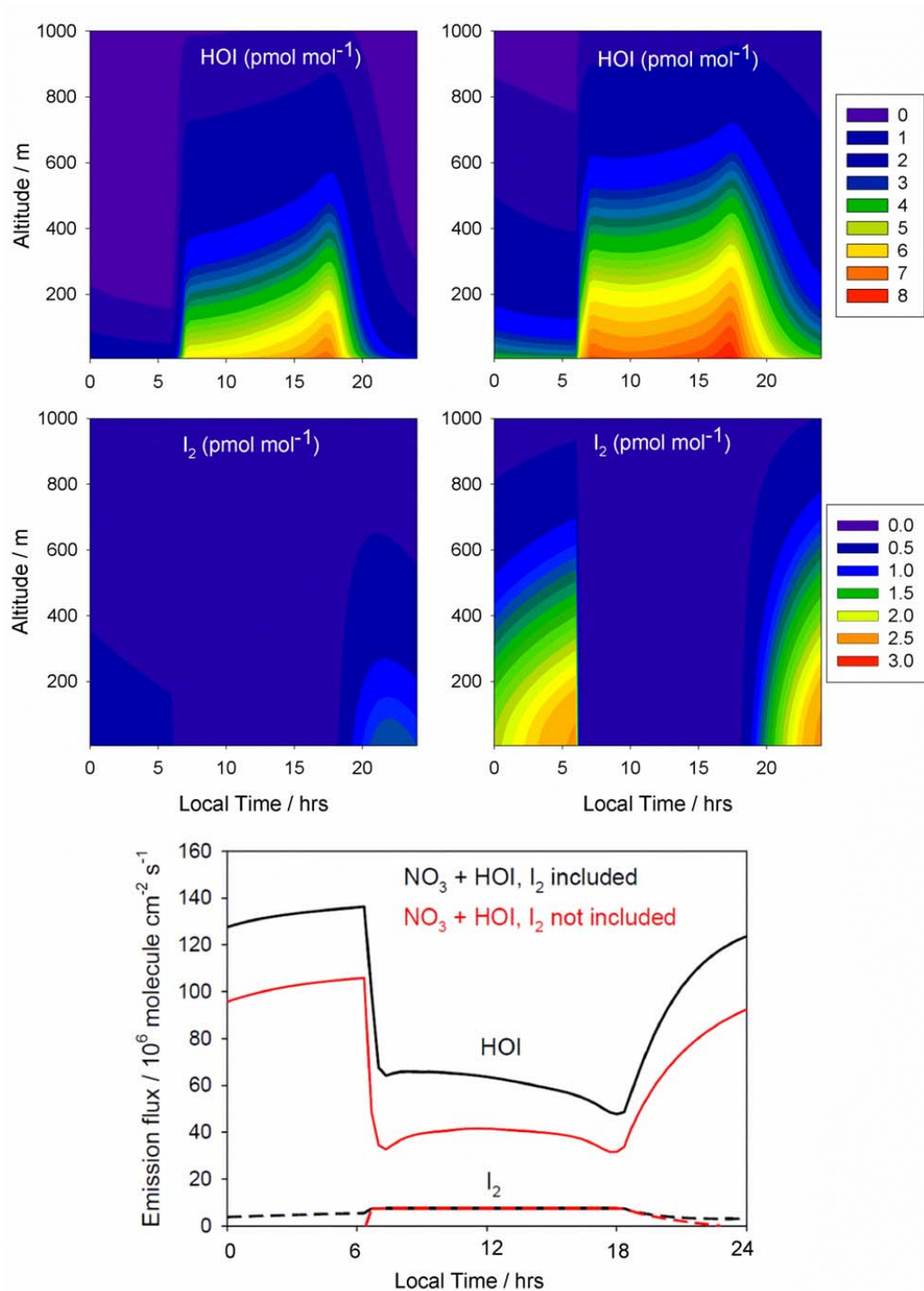
2

3

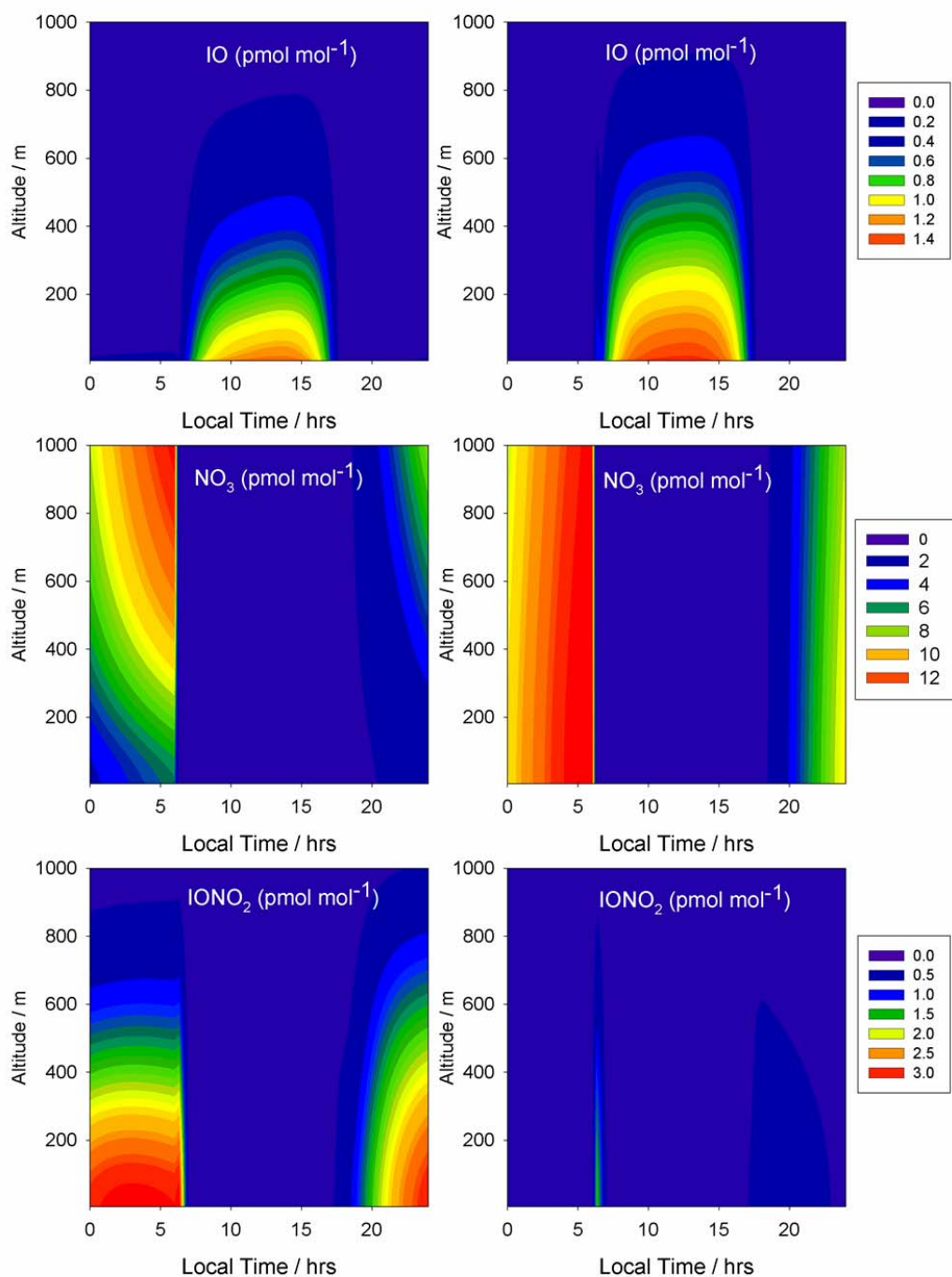
4 **Figure 3.** Potential energy surface for the reaction between HOI and NO<sub>3</sub>, which contains two  
5 intermediate complexes separated by a submerged barrier.

6

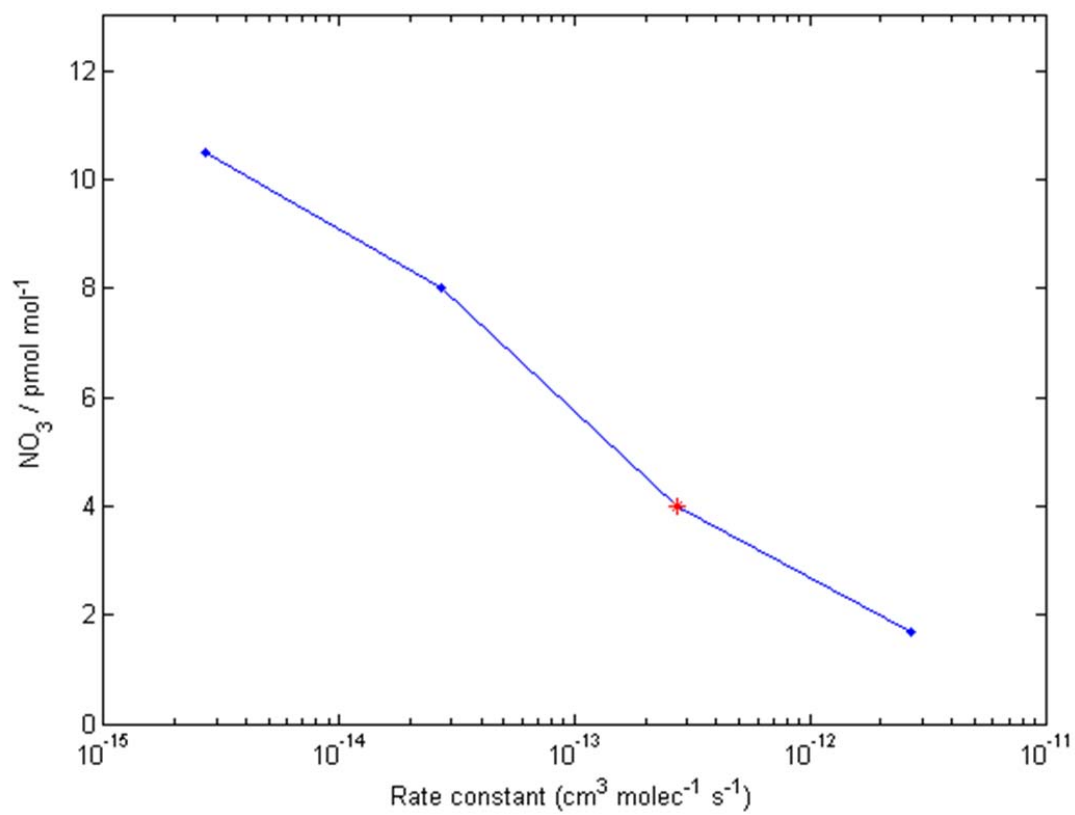




1  
 2 **Figure 4.** THAMO modeled diurnal variation of HOI, I<sub>2</sub> (upper panels) and the HOI/I<sub>2</sub> flux from  
 3 the ocean surface (bottom panel). The right hand panels are from scenario 1, which do not  
 4 include night time reactions of HOI and I<sub>2</sub> with NO<sub>3</sub>, while the left hand panels include the  
 5 reactions in scenario 2. In bottom panel red lines represent scenario 1, while black lines  
 6 correspond to scenario 2.



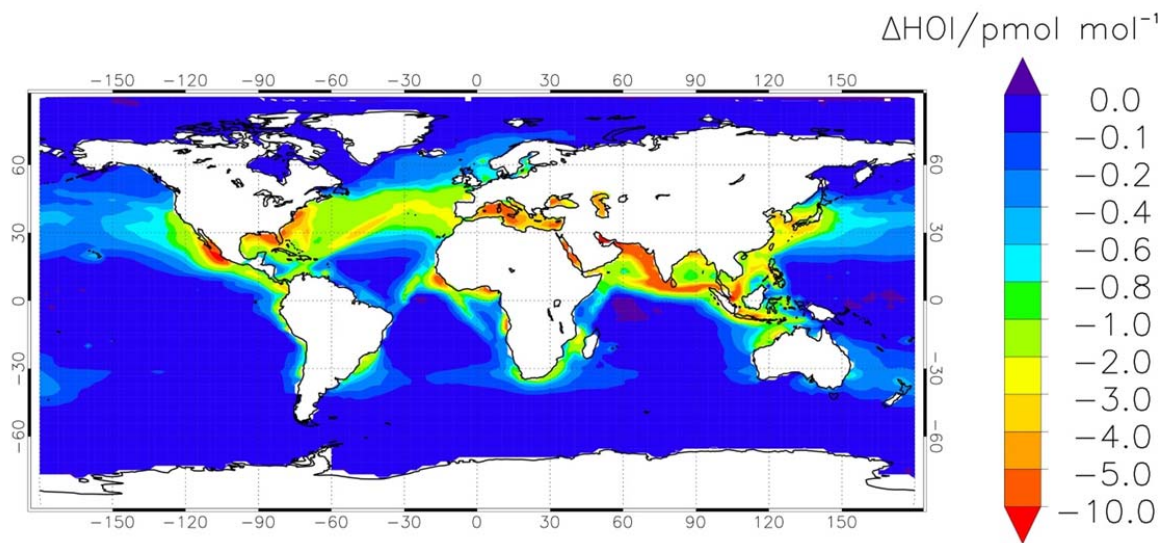
1  
 2 **Figure 5.** THAMO modeled diurnal variation of IO, NO<sub>3</sub> and the IONO<sub>2</sub>. The right hand panels  
 3 are from scenario 1, which do not include night time reactions of HOI and I<sub>2</sub> with NO<sub>3</sub>, while the  
 4 left hand panels include the reactions in scenario 2.



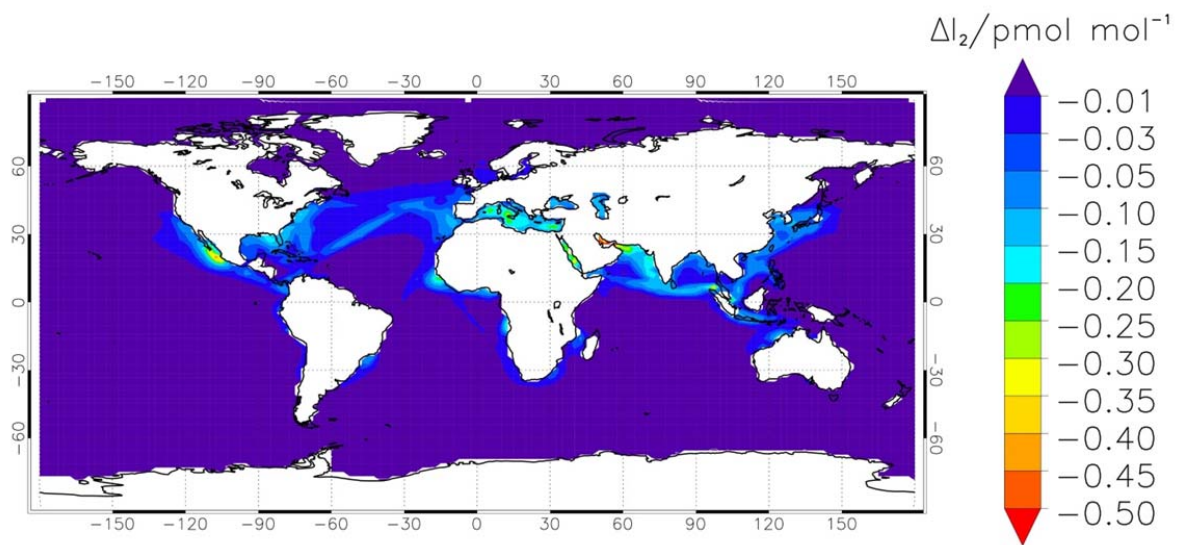
1  
2 **Figure 6.** Sensitivity run showing the effect of the uncertainty in the rate constant estimation on  
3 the reduction of NO<sub>3</sub> peak nighttime concentration at the surface - the red point is the theoretical  
4 estimate.

5  
6  
7  
8  
9  
10  
11

1



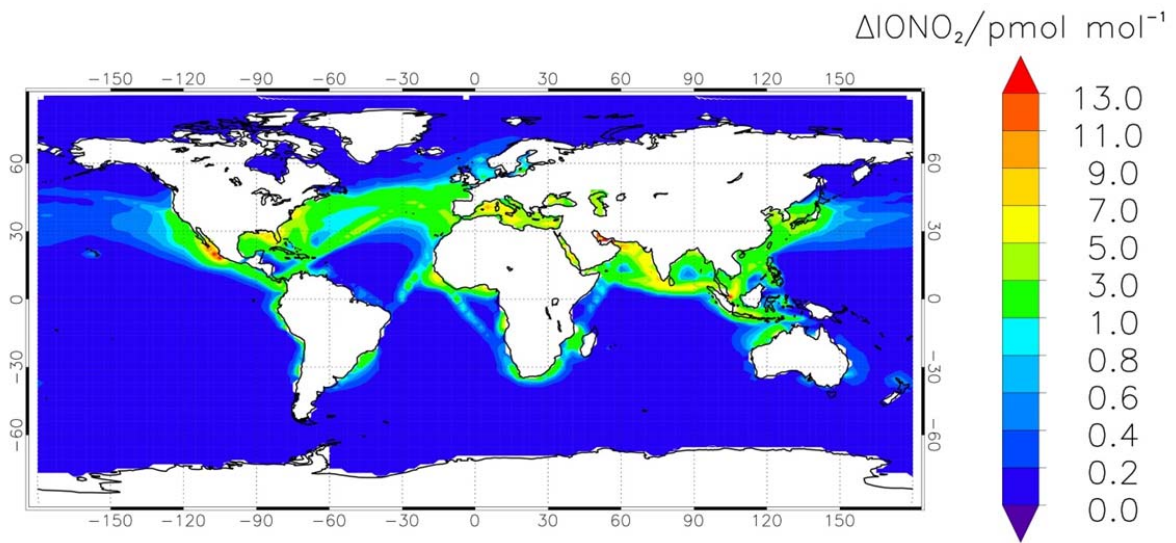
2



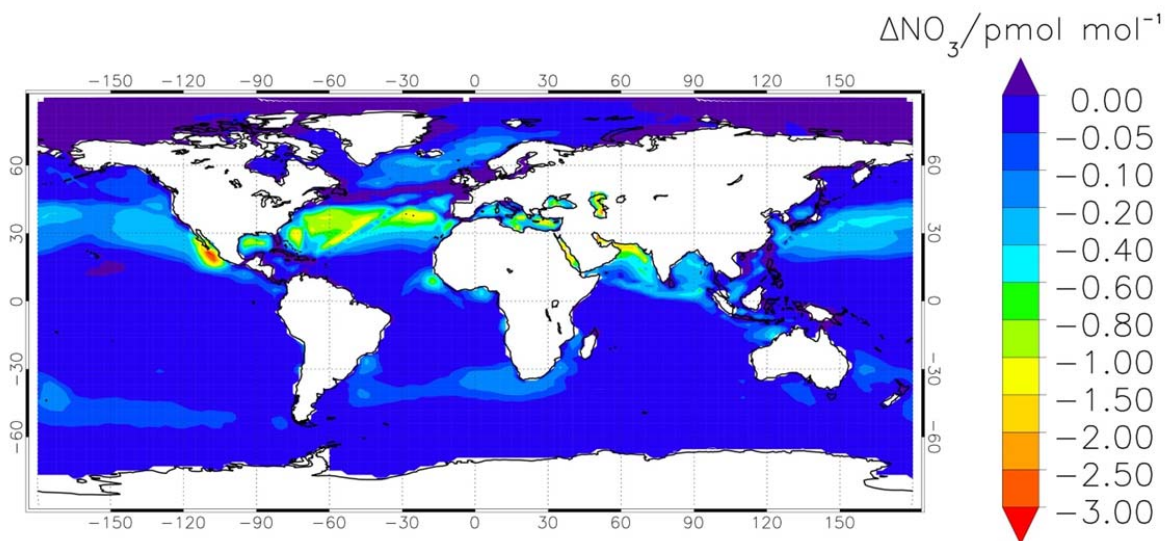
3

4 **Figure 7.** Modelled annual average of HOI (a) and I<sub>2</sub> (b) during night time (from 0:00 to 1:00  
5 LT) at the surface level. The panels show the difference in volume mixing ratio between the  
6 simulations with and without reactions (1) and (4).

7



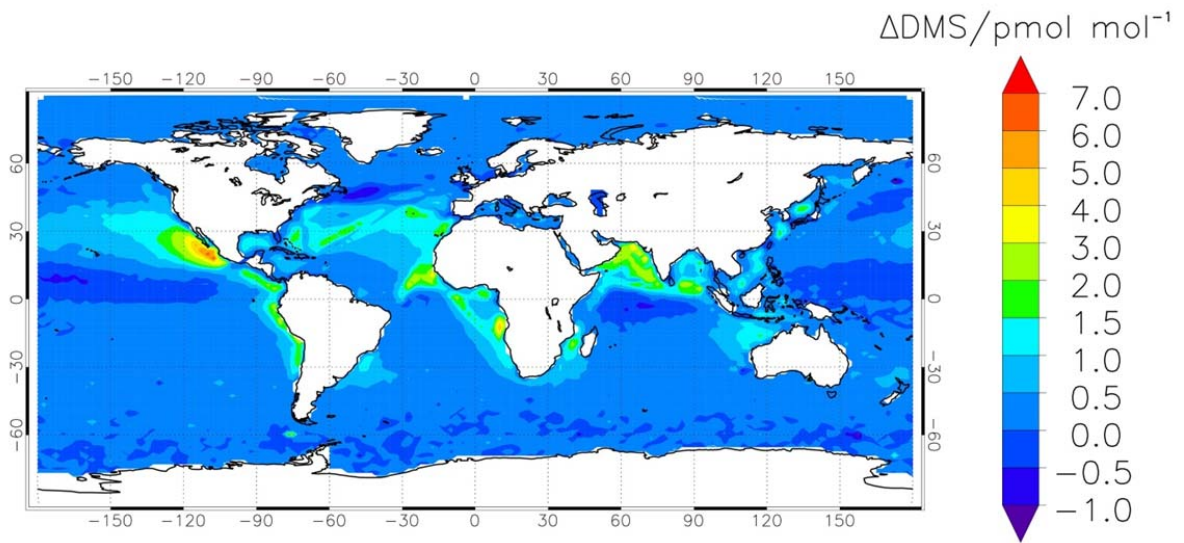
1



2

3 **Figure 8.** Modelled annual average of  $\text{IONO}_2$  (a) and  $\text{NO}_3$  (b) during night time (from 0:00 to  
4 1:00 LT) at the surface level, as the difference in volume mixing ratio between the simulations  
5 with and without reactions (1) and (4).

6



1

2 **Figure 9.** Increase in the DMS levels during night time (from 0:00 to 1:00 LT) at the surface  
3 level due to the inclusion of the reactions R1 and R4 in CAM-Chem.

4

5

6

7

8

9

10

11

12

13

14

15

16

1  
2  
3  
4  
5  
6  
7  
8  
9  
10  
11  
12  
13  
14  
15  
16  
17  
18  
19  
20  
21  
22  
23  
24

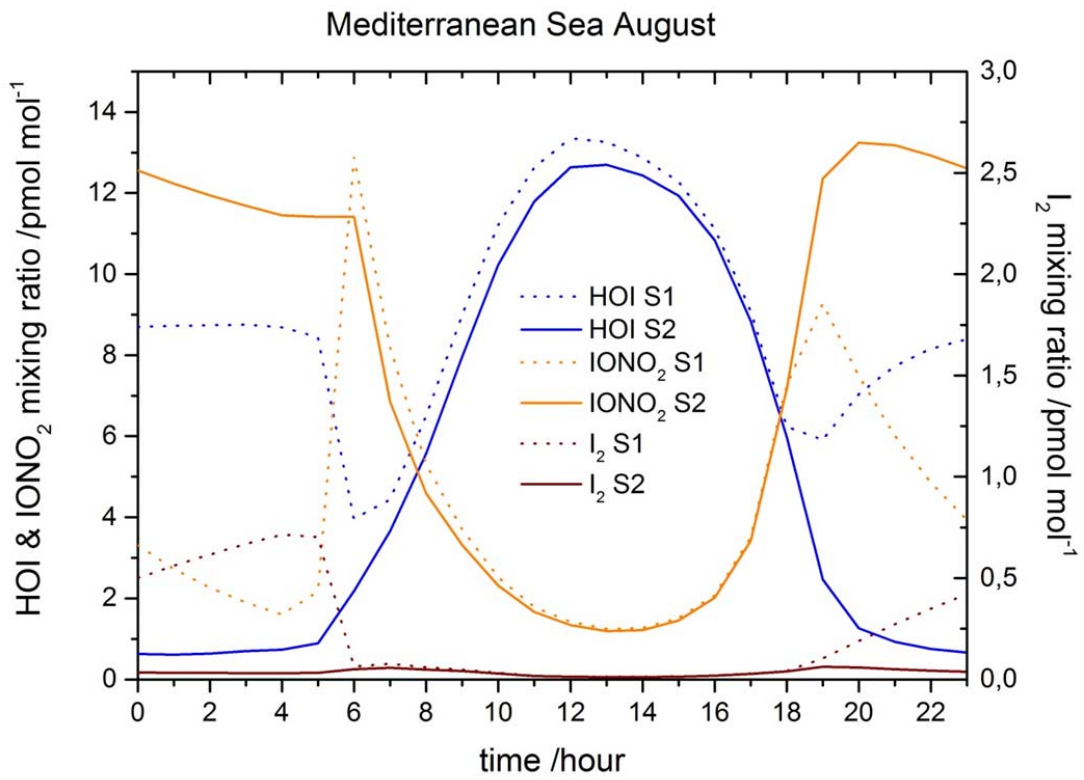
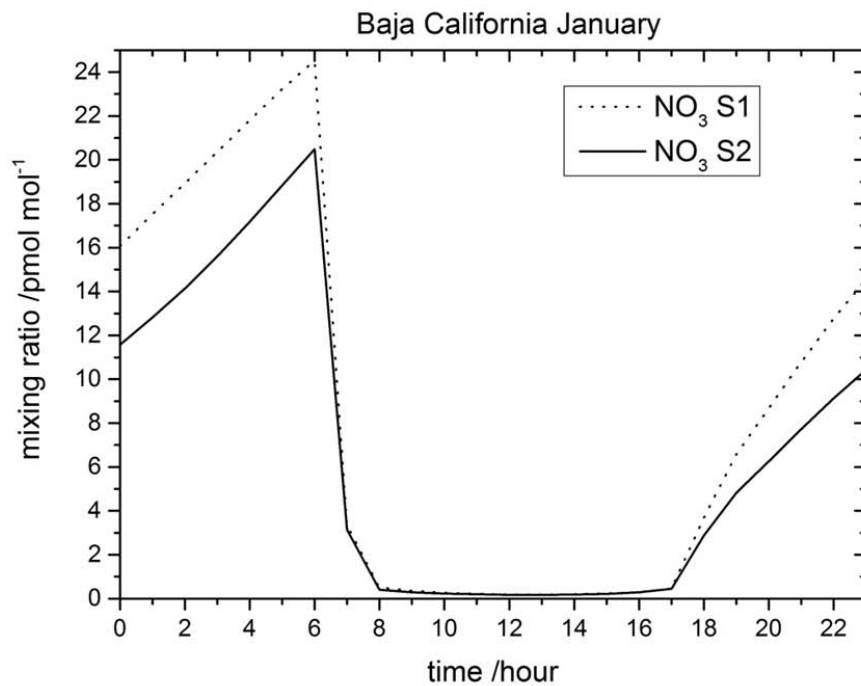
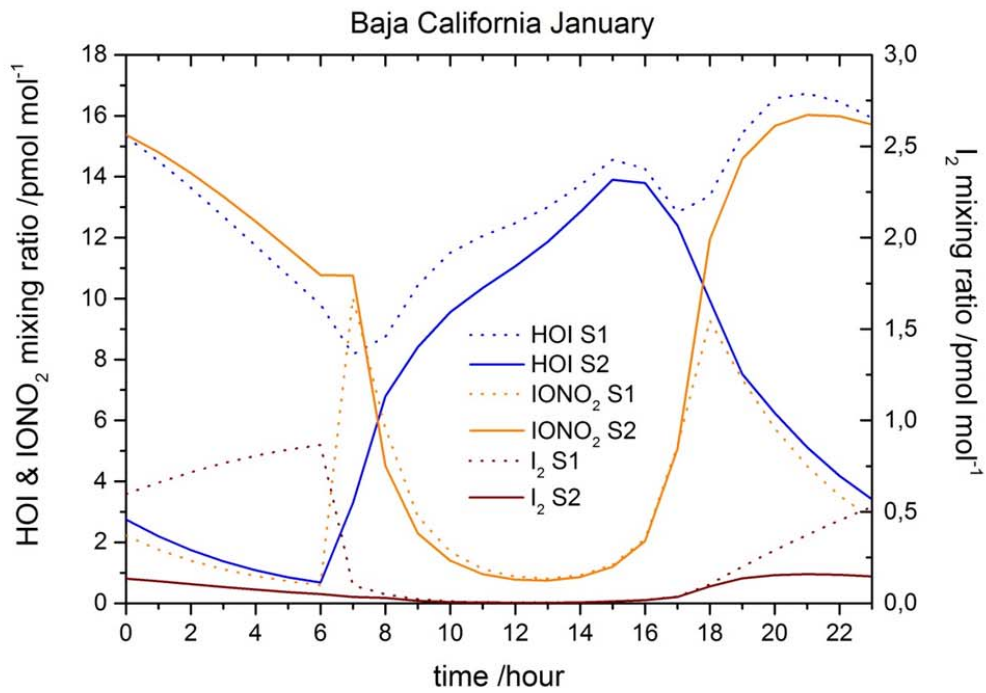


**Figure 10.** Hourly averaged concentration of HOI, IONO<sub>2</sub> and I<sub>2</sub> in the Mediterranean Sea at the surface level (lon:10°→20°E, lat:33°→40°N)



22 **Figure 11.** Hourly averaged concentration of HOI, IONO<sub>2</sub> and I<sub>2</sub> (upper panel) and NO<sub>3</sub> (bottom  
 23 panel) in the Pacific Ocean at the south of Baja California peninsula at the surface level  
 24 (lon: -110°→-106°E, lat:16°→23°N)



Supplementary information for

**Nighttime atmospheric chemistry of iodine**

Alfonso Saiz-Lopez<sup>1</sup>, John M.C. Plane<sup>2</sup>, Carlos A. Cuevas<sup>1</sup>, Anoop S. Mahajan<sup>3</sup>,  
Jean-François Lamarque<sup>4</sup> and Douglas E. Kinnison<sup>4</sup>

<sup>1</sup>Department of Atmospheric Chemistry and Climate, Institute of Physical Chemistry Rocasolano, CSIC, Madrid, Spain

<sup>2</sup>School of Chemistry, University of Leeds, Leeds, UK

<sup>3</sup>Indian Institute of Tropical Meteorology, Pune, India

<sup>4</sup>Atmospheric Chemistry Observations and Modelling, NCAR, Colorado, USA

Correspondence to: A. Saiz-Lopez (a.saiz@csic.es)

Table 1. Iodine chemistry scheme in CAM-Chem: Bimolecular, thermal decomposition and termolecular reactions.

Reaction	$k / \text{cm}^3 \text{ molecule}^{-1} \text{ s}^{-1}$	Notes
$\text{I} + \text{O}_3 \rightarrow \text{IO} + \text{O}_2$	$2.1 \times 10^{-11} e^{(-830/T)}$	1
$\text{IO} + \text{O}_3 \rightarrow \text{OIO} + \text{O}_2$	$3.6 \times 10^{-16}$	2
$\text{I} + \text{HO}_2 \rightarrow \text{HI} + \text{O}_2$	$1.5 \times 10^{-11} e^{(-1090/T)}$	3
$\text{IO} + \text{NO} \rightarrow \text{I} + \text{NO}_2$	$7.15 \times 10^{-12} e^{(300/T)}$	1
$\text{IO} + \text{HO}_2 \rightarrow \text{HOI} + \text{O}_2$	$1.4 \times 10^{-11} e^{(540/T)}$	1
$\text{IO} + \text{IO} \rightarrow \text{OIO} + \text{I}$	$2.13 \times 10^{-11} e^{(180/T)} \times [1 + e^{(p/191.42)}]$	1, 4
$\text{IO} + \text{IO} \rightarrow \text{I}_2\text{O}_2$	$3.27 \times 10^{-11} e^{(180/T)} \times [1 - 0.65 e^{(-p/191.42)}]$	1, 4
$\text{IO} + \text{OIO} \rightarrow \text{I}_2\text{O}_3$	$w_1 \cdot \exp(w_2 \cdot T)^a$	4, 5, 6 <sup>g</sup>
$\text{OIO} + \text{OIO} \rightarrow \text{I}_2\text{O}_4$	$w_1 \cdot \exp(w_2 \cdot T)^b$	4, 5, 6 <sup>g</sup>
$\text{I}_2 + \text{O} \rightarrow \text{IO} + \text{I}$	$1.25 \times 10^{-10}$	1
$\text{IO} + \text{O} \rightarrow \text{I} + \text{O}_2$	$1.4 \times 10^{-10}$	1
$\text{IO} + \text{OH} \rightarrow \text{HO}_2 + \text{I}$	$1.0 \times 10^{-10}$	7
$\text{I}_2\text{O}_2 \rightarrow \text{OIO} + \text{I}$	$w_1 \cdot \exp(w_2/T)^c$	5, 6, 8 <sup>g</sup>
$\text{I}_2\text{O}_2 \rightarrow \text{IO} + \text{IO}$	$w_1 \cdot \exp(w_2/T)^d$	5, 6, 8 <sup>g</sup>
$\text{I}_2\text{O}_4 \rightarrow 2 \text{OIO}$	$w_1 \cdot \exp(w_2/T)^e$	5, 8 <sup>g</sup>
$\text{I}_2 + \text{OH} \rightarrow \text{HOI} + \text{I}$	$1.8 \times 10^{-10}$	3
$\text{I}_2 + \text{NO}_3 \rightarrow \text{I} + \text{IONO}_2$	$1.5 \times 10^{-12}$	9
$\text{I} + \text{NO}_3 \rightarrow \text{IO} + \text{NO}_2$	$1.0 \times 10^{-10}$	1
$\text{OH} + \text{HI} \rightarrow \text{I} + \text{H}_2\text{O}$	$1.6 \times 10^{-11} e^{(440/T)}$	1
$\text{I} + \text{IONO}_2 \rightarrow \text{I}_2 + \text{NO}_3$	$9.1 \times 10^{-11} e^{(-146/T)}$	5
$\text{HOI} + \text{OH} \rightarrow \text{IO} + \text{H}_2\text{O}$	$2.0 \times 10^{-13}$	10
$\text{IO} + \text{DMS} \rightarrow \text{DMSO} + \text{I}$	$3.2 \times 10^{-13} e^{(-925/T)}$	11
$\text{INO}_2 \rightarrow \text{I} + \text{NO}_2$	$1008 \times 10^{15} e^{(-13670/T)}$	12, 13, 14
$\text{IONO}_2 \rightarrow \text{IO} + \text{NO}_2$	$w_1 \cdot \exp(w_2/T)^f$	5, 15
$\text{INO} + \text{INO} \rightarrow \text{I}_2 + 2\text{NO}$	$8.4 \times 10^{-11} e^{(-2620/T)}$	3
$\text{INO}_2 + \text{INO}_2 \rightarrow \text{I}_2 + 2\text{NO}_2$	$4.7 \times 10^{-13} e^{(-1670/T)}$	1
$\text{OIO} + \text{NO} \rightarrow \text{IO} + \text{NO}_2$	$1.1 \times 10^{-12} e^{(542/T)}$	14
$\text{HI} + \text{NO}_3 \rightarrow \text{I} + \text{HNO}_3$	$1.3 \times 10^{-12} e^{(-1830/T)}$	16
$\text{IO} + \text{BrO} \rightarrow \text{Br} + \text{I} + \text{O}_2$	$0.30 \times 10^{-11} e^{(510/T)}$	1
$\text{IO} + \text{BrO} \rightarrow \text{Br} + \text{OIO}$	$1.20 \times 10^{-11} e^{(510/T)}$	1
$\text{I} + \text{BrO} \rightarrow \text{IO} + \text{Br}$	$1.44 \times 10^{-11}$	17, 18, 19

$\text{IO} + \text{ClO} \rightarrow \text{I} + \text{OCIO}$	$2.585 \times 10^{-12} e^{(280/T)}$	1
$\text{IO} + \text{ClO} \rightarrow \text{I} + \text{Cl} + \text{O}_2$	$1.175 \times 10^{-12} e^{(280/T)}$	1
$\text{IO} + \text{ClO} \rightarrow \text{ICl} + \text{O}_2$	$0.940 \times 10^{-12} e^{(280/T)}$	1
$\text{IO} + \text{Br} \rightarrow \text{I} + \text{BrO}$	$2.49 \times 10^{-11}$	18, 19
$\text{IO} + \text{NO}_3 \rightarrow \text{OIO} + \text{NO}_2$	$9.0 \times 10^{-12}$	20
$\text{IO} + \text{CH}_3\text{O}_2 \rightarrow \text{CH}_2\text{O} + \text{I} + \text{HO}_2$	$2.0 \times 10^{-12}$	2 <sup>h</sup>
$\text{CH}_3\text{I} + \text{OH} \rightarrow \text{I} + \text{H}_2\text{O} + \text{HO}_2$	$2.90 \times 10^{-12} e^{(-1100/T)}$	3
$\text{I} + \text{NO}_2 (+ \text{M}) \rightarrow \text{INO}_2 (+ \text{M})$	$k_0 = 3 \times 10^{-31} \times (\text{T} / 300)^{-1}$ $k_\infty = 6.6 \times 10^{-11}$	3 <sup>i</sup>
$\text{IO} + \text{NO}_2 (+ \text{M}) \rightarrow \text{IONO}_2 (+ \text{M})$	$k_0 = 6.5 \times 10^{-31} \times (\text{T} / 300)^{-3.5}$ $k_\infty = 7.6 \times 10^{-12} \times (\text{T} / 300)^{-1.5}$	3 <sup>i</sup>
$\text{I} + \text{NO} (+ \text{M}) \rightarrow \text{INO} (+ \text{M})$	$k_0 = 1.8 \times 10^{-32} \times (\text{T} / 300)^{-1}$ $k_\infty = 1.7 \times 10^{-11}$	3 <sup>i</sup>
$\text{OIO} + \text{OH} (+ \text{M}) \rightarrow \text{HOIO}_2 (+ \text{M})$	$k_0 = 1.5 \times 10^{-27} \times (\text{T} / 300)^{-3.93}$ $k_\infty = 7.76 \times 10^{-10} \times (\text{T} / 300)^{-0.8}$	14 <sup>j</sup>
$\text{HOI} + \text{NO}_3 \rightarrow \text{IO} + \text{HNO}_3$	$2.7 \times 10^{-12} (300/\text{T})^{2.66}$	21

<sup>1</sup> IUPAC-2008 (Atkinson et al., 2007) ; <sup>2</sup>(Dillon et al., 2006b); <sup>3</sup> JPL-2010 (Sander et al., 2011); <sup>4</sup>(Gómez Martín et al., 2007); <sup>5</sup>(Kaltsoyannis and Plane, 2008); <sup>6</sup>(Galvez et al., 2013); <sup>7</sup>(Bösch et al., 2003); <sup>8</sup> (Gómez Martín and Plane, 2009); <sup>9</sup>(Chambers et al., 1992); <sup>10</sup>(Chameides and Davis, 1980); <sup>11</sup>(Dillon et al., 2006a); <sup>12</sup>(McFiggans et al., 2000); <sup>13</sup>(Jenkin et al., 1985); <sup>14</sup>(Plane et al., 2006); <sup>15</sup>(Allan and Plane, 2002); <sup>16</sup>(Lancar et al., 1991); <sup>17</sup>(Laszlo et al., 1997); <sup>18</sup>(Bedjanian et al., 1997); <sup>19</sup>(Gilles et al., 1997); <sup>20</sup>(Dillon et al., 2008); <sup>21</sup>This work.

$$^a \quad w1 = 4.687 \times 10^{-10} - 1.3855 \times 10^{-5} \times e^{(-0.75 \text{ p} / 1.62265)} + 5.51868 \times 10^{-10} \times e^{(-0.75 \text{ p} / 199.328)}$$

$$w2 = -0.00331 - 0.00514 \times e^{(-0.75 \text{ p} / 325.68711)} - 0.00444 \times e^{(-0.75 \text{ p} / 40.81609)}$$

$$^b \quad w1 = 1.1659 \times 10^{-9} - 7.79644 \times 10^{-10} \times e^{(-0.75 \text{ p} / 22.09281)} + 1.03779 \times 10^{-9} \times e^{(-0.75 \text{ p} / 568.15381)}$$

$$w2 = -0.00813 - 0.00382 \times e^{(-0.75 \text{ p} / 45.57591)} - 0.00643 \times e^{(-0.75 \text{ p} / 417.95061)}$$

$$^c \quad w1 = 3.54288 \times 10^{10} + 1.8523 \times 10^{11} \times 0.75 \text{ p} - 1.45435 \times 10^8 \times (0.75 \text{ p})^2 + 60799.4344 \times (0.75 \text{ p})^3$$

$$w2 = -9681.65989 + 346.95538 \times e^{(-0.75 \text{ p} / 343.25322)} + 251.78032 \times e^{(-0.75 \text{ p} / 44.1466)}$$

$$^d \quad w1 = 255335000000 - 4418880000 \times 0.75 \text{ p} + 85618600 \times (0.75 \text{ p})^2 + 14218.81 \times (0.75 \text{ p})^3$$

$$w2 = -11466.82304 + 597.01334 \times e^{(-0.75 \text{ p} / 1382.62325)} - 167.3391 \times e^{(-0.75 \text{ p} / 43.75089)}$$

$$^e \quad w1 = -1.92626 \times 10^{14} + 4.67414 \times 10^{13} \times 0.75 \text{ p} - 3.68651 \times 10^8 \times (0.75 \text{ p})^2 - 3.09109 \times 10^6 \times (0.75 \text{ p})^3$$

$$w2 = -12302.15294 + 252.78367 \times e^{(-0.75 \text{ p} / 46.12733)} + 437.62868 \times e^{(-0.75 \text{ p} / 428.4413)}$$

$$\begin{aligned}
 {}^f \quad w_1 &= -2.63544 \times 10^{13} + 4.32845 \times 10^{12} \times (0.75 \text{ p}) + 3.73758 \times 10^8 \times (0.75 \text{ p})^2 - \\
 &628468.76313 \times (0.75 \text{ p})^3 \\
 w_2 &= -13847.85015 + 240.34465 \times e^{(-0.75 \text{ p} / 49.27141)} + 451.35864 \times e^{(-0.75 \text{ p} / \\
 &436.87605)}
 \end{aligned}$$

<sup>g</sup> The empirical expressions of the form  $w_1 \cdot \exp(w_2 \cdot T)$  were obtained by non-linear least squares fitting of *Rice–Ramsperger–Kassel–Marcus* (RRKM) theoretical results for the indicated reaction rate constants and thermal dissociation rates in the (27 – 1013) hPa pressure range. RRKM calculations were carried out using the MESMER algorithm (Glowacki et al., 2012) as indicated in the corresponding references (e.g. (Galvez et al., 2013)). Expression <sup>a</sup> produces negative values outside the range of modelled rate constants ( $p < 20$  hPa), and therefore a fixed rate constant of  $3 \times 10^{-11} \text{ cm}^3 \text{ molecule}^{-1} \text{ s}^{-1}$  was assumed. Expressions <sup>e</sup> and <sup>f</sup> generate negligible dissociation rates below  $\sim 500$  hPa which become negative at  $\sim 8$  hPa – in this case they are set to zero below that pressure.

<sup>h</sup> Updated heats of formation for IO, OIO, and  $\text{CH}_3\text{O}_2$  (Dooley et al., 2008; Gómez Martín and Plane, 2009; Knyazev and Slagle, 1998) show that the only accessible exothermic product channel of  $\text{CH}_3\text{O}_2 + \text{IO}$  (Drougas and Kosmas, 2007) is  $\text{CH}_2\text{O} + \text{I} + \text{O}_2$  ( $\Delta H_r = -5 \pm 6 \text{ kJ mol}^{-1}$ ), consistent with the high yield of I and low yield of OIO found experimentally (Bale et al., 2005; Enami et al., 2006). Sensitivity studies have been carried out (Saiz-Lopez et al., 2014) using the preferred rate constant for this reaction of  $2 \times 10^{-12} \text{ cm}^3 \text{ molecule}^{-1} \text{ s}^{-1}$  (Dillon et al., 2006b), resulting in an enhancement of the ozone loss of 0.5% in the MBL and of less than 0.1% integrated throughout the troposphere in the  $J_{\text{I}_x\text{O}_y}$  scenario, and similarly negligible enhancements in the Base scenario. Impacts in the  $I_y$  partitioning are also very minor.

<sup>i</sup> The temperature and pressure dependent rate constant ( $k$ ) is computed based on the low pressure ( $k_0$ ) and the high-pressure ( $k_\infty$ ) rate coefficients following JPL-2010 (Sander et al., 2011).

<sup>j</sup> The Fast rate constants and a thermally stable product  $\text{HOIO}_2$  have been predicted theoretically (Plane et al., 2006), but no experimental studies reporting observation of  $\text{HOIO}_2$  and its photochemical properties in the gas phase are available. Since the level of uncertainty is even larger than for the  $\text{I}_x\text{O}_y$ , it has not been included in the mechanism.

Table 2. Iodine chemistry scheme in CAM-Chem: Photochemical reactions.

Reaction
$\text{CH}_3\text{I} + h\nu \rightarrow \text{CH}_3\text{O}_2 + \text{I}$
$\text{CH}_2\text{I}_2 + h\nu \rightarrow 2\text{I}^a$
$\text{CH}_2\text{IBr} + h\nu \rightarrow \text{Br} + \text{I}^a$
$\text{CH}_2\text{ICl} + h\nu \rightarrow \text{Cl} + \text{I}^a$
$\text{I}_2 + h\nu \rightarrow 2\text{I}$
$\text{IO} + h\nu \rightarrow \text{I} + \text{O}$
$\text{OIO} + h\nu \rightarrow \text{I} + \text{O}_2$
$\text{INO} + h\nu \rightarrow \text{I} + \text{NO}$
$\text{INO}_2 + h\nu \rightarrow \text{I} + \text{NO}_2^b$
$\text{IONO}_2 + h\nu \rightarrow \text{I} + \text{NO}_3$
$\text{HOI} + h\nu \rightarrow \text{I} + \text{OH}$
$\text{IBr} + h\nu \rightarrow \text{I} + \text{Br}$
$\text{ICl} + h\nu \rightarrow \text{I} + \text{Cl}$
$\text{I}_2\text{O}_2 + h\nu \rightarrow \text{I} + \text{OIO}^c$
$\text{I}_2\text{O}_3 + h\nu \rightarrow \text{IO} + \text{OIO}^c$
$\text{I}_2\text{O}_4 + h\nu \rightarrow \text{OIO} + \text{OIO}^c$

Photolysis rates are computed online considering the actinic flux calculation in CAM-Chem. The absorption cross-sections and quantum yields for all species besides the  $\text{I}_x\text{O}_y$  have been taken from IUPAC-2008 (Atkinson et al., 2007; Atkinson et al., 2008) and JPL-2010 (Sander et al., 2011).

<sup>a</sup> radical organic products are not considered.

<sup>b</sup> only the reaction channel reported in JPL 06-02 (Sander et al., 2006) is considered.

<sup>c</sup> photolysis reactions only considered in the  $J_{\text{I}x\text{O}y}$  scheme (Saiz-Lopez et al., 2014).

Table 3. Iodine chemistry scheme in CAM-Chem: Heterogeneous reactions.

<b>Sea-salt aerosol reactions</b>	<b>Reactive uptake</b>
$\text{IONO}_2 \rightarrow 0.5 \text{ IBr} + 0.5 \text{ ICl}$	$\gamma = 0.01$
$\text{INO}_2 \rightarrow 0.5 \text{ IBr} + 0.5 \text{ ICl}$	$\gamma = 0.02$
$\text{HOI} \rightarrow 0.5 \text{ IBr} + 0.5 \text{ ICl}$	$\gamma = 0.06$
$\text{I}_2\text{O}_2 \rightarrow$	$\gamma = 0.01^{\S}$
$\text{I}_2\text{O}_3 \rightarrow$	$\gamma = 0.01^{\S}$
$\text{I}_2\text{O}_4 \rightarrow$	$\gamma = 0.01^{\S}$

Values based on the THAMO model (Saiz-Lopez et al., 2008) and implemented in CAM-Chem following (Ordóñez et al., 2012).

<sup>§</sup> Deposition of  $\text{I}_x\text{O}_y$  species on sea-salt aerosols has been included following the free regime approximation.

Table 4. Iodine chemistry scheme in CAM-Chem: Henry's Law constants and dry deposition velocities.

Species	$k_0$ (M atm <sup>-1</sup> )	Deposition velocity <sup>§</sup> (cm s <sup>-1</sup> )	Reference
IBr <sup>ice</sup>	$2.4 \times 10^1$	–	1
ICl <sup>ice</sup>	$1.1 \times 10^2$	–	1
HI	$7.8 \times 10^{-1}$	1.0	1 <sup>a</sup>
HOI – ( $J_{I_xO_y} / Base$ )	$1.9 \times 10^3 / 4.5 \times 10^3$	0.75	1 <sup>b</sup>
IONO <sub>2</sub> <sup>ice</sup>	$1.0 \times 10^6$	0.75	2 <sup>c</sup>
INO <sub>2</sub> <sup>ice</sup>	$3.0 \times 10^{-1}$	0.75	1 <sup>d</sup>
IO	$4.5 \times 10^2$	–	2
OIO	$1.0 \times 10^4$	–	2
I <sub>2</sub> O <sub>2</sub>	$1.0 \times 10^4$	1.0	2
I <sub>2</sub> O <sub>3</sub>	$1.0 \times 10^4$	1.0	2
I <sub>2</sub> O <sub>4</sub>	$1.0 \times 10^4$	1.0	2

<sup>§</sup> Dry deposition velocities are based on the THAMO model (Saiz-Lopez et al., 2008).

<sup>1</sup> Values reported in (Sander, 1999).

<sup>2</sup> Values based on the THAMO model (Saiz-Lopez et al., 2008).

<sup>a</sup> Considering a dissociation constant  $K_a = 3.2 \times 10^9$  and a temperature dependent coefficient  $c = 9800$  K

<sup>b</sup> Within the range of values given in the corresponding reference.

<sup>c</sup> Virtually infinite solubility is represented by using a very large arbitrary number.

<sup>d</sup> Value assumed to be equal to those of BrNO<sub>2</sub>.

<sup>ice</sup> Species for which ice-uptake is considered following (Neu and Prather, 2012).

## References

Allan, B. J., and Plane, J. M. C.: A Study of the Recombination of IO with NO<sub>2</sub> and the Stability of INO<sub>3</sub>: Implications for the Atmospheric Chemistry of Iodine, *J. Phys. Chem. A*, 106, 8634-8641, 2002.

Atkinson, R., Baulch, D. L., Cox, R. A., Crowley, J. N., Hampson, R. F., Hynes, R. G., Jenkin, M. E., Rossi, M. J., and Troe, J.: Evaluated kinetic and photochemical data for atmospheric chemistry: Volume III: gas phase reactions of inorganic halogens, *Atmos. Chem. Phys.*, 7, 981-1191, 2007.

Atkinson, R., Baulch, D. L., Cox, R. A., Crowley, J. N., Hampson, R. F., Hynes, R. G., Jenkin, M. E., Rossi, M. J., Troe, J., and Wallington, T. J.: Evaluated kinetic and photochemical data for atmospheric chemistry: Volume IV – gas phase reactions of organic halogen species, *Atmos. Chem. Phys.*, 8, 4141-4496, 10.5194/acp-8-4141-2008, 2008.

- Bale, C. S. E., Canosa-Mas, C. E., Shallcross, D. E., and Wayne, R. P.: A discharge-flow study of the kinetics of the reactions of IO with CH<sub>3</sub>O<sub>2</sub> and CF<sub>3</sub>O<sub>2</sub>, *Phys. Chem. Chem. Phys.*, 7, 2164-2172, 2005.
- Bedjanian, Y., Le Bras, G., and Poulet, G.: Kinetic study of the Br + IO, I + BrO and Br + I<sub>2</sub> reactions. Heat of formation of the BrO radical, *Chem. Phys. Lett.*, 266, 233-238, doi: 10.1016/S0009-2614(97)01530-3, 1997.
- Bösch, H., Camy-Peyret, C., Chipperfield, M. P., Fitzenberger, R., Harder, H., Platt, U., and Pfeilsticker, K.: Upper limits of stratospheric IO and OIO inferred from center-to-limb-darkening-corrected balloon-borne solar occultation visible spectra: Implications for total gaseous iodine and stratospheric ozone, *J. Geophys. Res.*, 108, 4455, 2003.
- Chambers, R. M., Heard, A. C., and Wayne, R. P.: Inorganic gas-phase reactions of the nitrate radical: iodine + nitrate radical and iodine atom + nitrate radical, *J. Phys. Chem.*, 96, 3321-3331, 10.1021/j100187a028, 1992.
- Chameides, W. L., and Davis, D.: Iodine: Its Possible Role in Tropospheric Photochemistry, *J. Geophys. Res.*, 85, 7383-7398, 1980.
- Dillon, T. J., Karunanandan, R., and Crowley, J. N.: The reaction of IO with CH<sub>3</sub>SCH<sub>3</sub>: products and temperature dependent rate coefficients by laser induced fluorescence, *Phys. Chem. Chem. Phys.*, 8, 847-855, 2006a.
- Dillon, T. J., Tucceri, M. E., and Crowley, J. N.: Laser induced fluorescence studies of iodine oxide chemistry Part II. The reactions of IO with CH<sub>3</sub>O<sub>2</sub>, CF<sub>3</sub>O<sub>2</sub> and O<sub>3</sub>., *Phys. Chem. Chem. Phys.*, 8, 5185-5198, 2006b.
- Dillon, T. J., Tucceri, M. E., Sander, R., and Crowley, J. N.: LIF studies of iodine oxide chemistry Part 3. Reactions IO + NO<sub>3</sub> -> OIO + NO<sub>2</sub>, I + NO<sub>3</sub> -> IO + NO<sub>2</sub>, and CH<sub>2</sub>I + O<sub>2</sub> -> (products): implications for the chemistry of the marine atmosphere at night., *Phys. Chem. Chem. Phys.*, 10, 1540-1554, 2008.
- Dooley, K. S., Geidosch, J. N., and North, S. W.: Ion imaging study of IO radical photodissociation: Accurate bond dissociation energy determination, *Chem. Phys. Lett.*, 457, 303-306, 2008.
- Drougas, E., and Kosmas, A. M.: Ab Initio Characterization of (CH<sub>3</sub>IO<sub>3</sub>) Isomers and the CH<sub>3</sub>O<sub>2</sub> + IO Reaction Pathways, *J. Phys. Chem. A*, 111, 3402-3408, 2007.
- Enami, S., Yamanaka, T., Hashimoto, S., Kawasaki, M., Nakano, Y., and Ishiwata, T.: Kinetic Study of IO Radical with RO<sub>2</sub> (R = CH<sub>3</sub>, C<sub>2</sub>H<sub>5</sub>, and CF<sub>3</sub>) Using Cavity Ring-Down Spectroscopy, *J. Phys. Chem. A*, 110, 9861-9866, 2006.
- Galvez, O., Gomez Martin, J. C., Gomez, P. C., Saiz-Lopez, A., and Pacios, L. F.: A theoretical study on the formation of iodine oxide aggregates and monohydrates, *Phys. Chem. Chem. Phys.*, 15, 15572-15583, 10.1039/C3CP51219C, 2013.
- Gilles, M. K., Turnipseed, A. A., Burkholder, J. B., and Ravishankara, A. R.: A study of the Br + IO → I + BrO and the reverse reaction, *Chem. Phys. Lett.*, 272, 75-82, doi: 10.1016/S0009-2614(97)00485-5, 1997.
- Glowacki, D. R., Liang, C.-H., Morley, C., Pilling, M. J., and Robertson, S. H.: MESMER: An Open-Source Master Equation Solver for Multi-Energy Well Reactions, *J. Phys. Chem. A*, 116, 9545-9560, 10.1021/jp3051033, 2012.
- Gómez Martín, J. C., Spietz, P., and Burrows, J. P.: Kinetic and Mechanistic Studies of the I<sub>2</sub>/O<sub>3</sub> Photochemistry, *J. Phys. Chem. A*, 111, 306-320, 2007.



- Gómez Martín, J. C., and Plane, J. M. C.: Determination of the O-IO bond dissociation energy by photofragment excitation spectroscopy, *Chem. Phys. Lett.*, 474, 79-83, 2009.
- Jenkin, M. E., Cox, R. A., and Candeland, D. E.: Photochemical Aspects of Tropospheric Iodine Behavior, *J. Atmos. Chem.*, 2, 359-375, 1985.
- Kaltsoyannis, N., and Plane, J. M. C.: Quantum chemical calculations on a selection of iodine-containing species (IO, OIO,  $\text{INO}_3$ ,  $(\text{IO})_2$ ,  $\text{I}_2\text{O}_3$ ,  $\text{I}_2\text{O}_4$  and  $\text{I}_2\text{O}_5$ ) of importance in the atmosphere., *Phys. Chem. Chem. Phys.*, 10, 1723-1733, 2008.
- Knyazev, V. D., and Slagle, I. R.: Thermochemistry of the R-O2 Bond in Alkyl and Chloroalkyl Peroxy Radicals, *J. Phys. Chem. A*, 102, 1770-1778, 10.1021/jp9726091, 1998.
- Lancar, I. T., Mellouki, A., and Poulet, G.: Kinetics of the reactions of hydrogen iodide with hydroxyl and nitrate radicals, *Chem. Phys. Lett.*, 177, 554-558, 1991.
- Laszlo, B., Huie, R. E., Kurylo, M. J., and Miziolek, A. W.: Kinetic studies of the reactions of BrO and IO radicals, *J. Geophys. Res.*, 102, 1997.
- McFiggans, G., Plane, J. M. C., Allan, B. J., Carpenter, L. J., Coe, H., and O'Dowd, C.: A modeling study of iodine chemistry in the marine boundary layer, *J. Geophys. Res.*, [Atmos.], 105, 14371-14385, 2000.
- Neu, J. L., and Prather, M. J.: Toward a more physical representation of precipitation scavenging in global chemistry models: cloud overlap and ice physics and their impact on tropospheric ozone, *Atmos. Chem. Phys.*, 12, 3289-3310, 10.5194/acp-12-3289-2012, 2012.
- Ordóñez, C., Lamarque, J. F., Tilmes, S., Kinnison, D. E., Atlas, E. L., Blake, D. R., Sousa Santos, G., Brasseur, G., and Saiz-Lopez, A.: Bromine and iodine chemistry in a global chemistry-climate model: description and evaluation of very short-lived oceanic sources, *Atmos. Chem. Phys.*, 12, 1423-1447, 10.5194/acp-12-1423-2012, 2012.
- Plane, J. M. C., Joseph, D. M., Allan, B. J., Ashworth, S. H., and Francisco, J. S.: An Experimental and Theoretical Study of the Reactions  $\text{OIO} + \text{NO}$  and  $\text{OIO} + \text{OH}$ , *J. Phys. Chem. A*, 110, 93-100, 2006.
- Saiz-Lopez, A., Plane, J. M. C., Mahajan, A. S., Anderson, P. S., Bauguitte, S. J.-B., Jones, A. E., Roscoe, H. K., Salmon, R. A., Bloss, W. J., Lee, J. D., and Heard, D. E.: On the vertical distribution of boundary layer halogens over coastal Antarctica: implications for  $\text{O}_3$ ,  $\text{HO}_x$ ,  $\text{NO}_x$  and the Hg lifetime, *Atmos. Chem. Phys.*, 8, 887-900, 2008.
- Saiz-Lopez, A., Fernandez, R. P., Ordóñez, C., Kinnison, D. E., Gómez Martín, J. C., Lamarque, J. F., and Tilmes, S.: Iodine chemistry in the troposphere and its effect on ozone, *Atmos. Chem. Phys.*, 14, 13119-13143, 10.5194/acp-14-13119-2014, 2014.
- Sander, R.: Compilation of Henry's Law Constants for Inorganic and Organic Species of Potential Importance in Environmental Chemistry (v3), available at: <http://www.henrys-law.org/> (last access: 1 Sept 2016), 1999.
- Sander, S. P., Friedl, R. R., Golden, D. M., Kurylo, M. J., Moortgat, G. K., Wine, P. H., Ravishankara, A. R., Kolb, C. E., Molina, M. J., Diego, S., Jolla, L., Huie, R. E., and Orkin, V. L.: Chemical Kinetics and Photochemical Data for Use in Atmospheric Studies Evaluation Number 15, JPL\_NASA, 06-2, Jet Propulsion Laboratory, Pasadena, CA, 2006.

Sander, S. P., Friedl, R. R., Barker, J. R., Golden, D. M., Kurylo, M. J., Sciences, G. E., Wine, P. H., Abbatt, J. P. D., Burkholder, J. B., Kolb, C. E., Moortgat, G. K., Huie, R. E., and Orkin, V. L.: Chemical Kinetics and Photochemical Data for Use in Atmospheric Studies, Evaluation No. 17, JPL\_NASA, 10-6, Jet Propulsion Laboratory, Pasadena, CA, 2011.